R. & M. No. 2074
(6932)
A.R.C. Technical Report

MINISTRY OF AIRCRAFT PRODUCTION

AERONAUTICAL RESEARCH COUNCIL
REPORTS AND MEMORANDA

# Lateral Stability of Tailless Aircraft

*By*

A. W. Thorpe, B.A. and M. F. Curtis



LONDON: HIS MAJESTY'S STATIONERY OFFICE
1948
Price 5*s.* 6*d.* net

# Lateral Stability of Tailless Aircraft

*By*

A. W. Thorpe, B.A. and M. F. Curtis

Communicated by the Director-General of Scientific Research,
Ministry of Aircraft Production

*Reports and Memoranda No.* 2074

*June,* 1943*

*Summary.—Reasons for Enquiry.*—Information was required on the probable effect on lateral behaviour of a change from conventional to tailless types.

*Range of Investigations.*—The essential features of a tailless design are represented by large reductions in the absolute values of the derivatives $y_v$, $n_v$, $n_r$. As few tailless models have been studied, a numerical survey of stability boundaries has been made over a range of these parameters which probably covers the limits set by the all-wing design without end fins.

Curves of constant period and constant damping have been drawn in a few cases and from these curves a numerical comparison of the stability characteristics of conventional and tailless aircraft has been made.

*Conclusions.*—(1) For the larger values of $n_r$ and $y_v$ considered, oscillatory instability is more likely to occur at low speed than at high, and instability at high speed is unlikely. For the smaller values of $n_r$ and $y_v$, oscillatory instability is more likely at high speed than at low speed, and stability at high speed can be attained only with a small value of $-l_v$.

(2) Spiral instability is probable at all speeds, but at high speed the rate of growth of this motion will be small.

(3) The survey stresses the need for systematic measurements of $y_v$, $n_v$, $n_r$ (particularly the last) in the tailless range.

1. *Introduction.*—Lateral stability characteristics have been investigated previously (R. & M. 1989[1, 2]) but such investigations have been concerned mainly with the conventional type of aircraft, where it was possible with fair approximation to use standard values for most of the aerodynamic derivatives. In order to examine the lateral behaviour of tailless aircraft, similar calculations have been made using the range of values likely to occur in aircraft of this type.

Attention has been paid chiefly to the case of the true flying wing with no fins. In this case there is no linear relation between $n_v$ and $n_r$ and it is necessary to treat these as independent variables. For a wing with end fins there will be a relation of the form $n_r = a + bn_v$, but the quantities $a$ and $b$ can have such a wide range of values that exploration on these lines would be impractical. If $n_v$ and $n_r$ are assumed to be unrelated then we can take $\mu n_v$ and $-\mu l_v$ as independent variables for plotting stability diagrams, and variation of the boundary with $\mu$ is then eliminated.

It is considered that in a tailless aircraft without fins, the values of $-n_r$ and $n_v$ are unlikely to exceed $0 \cdot 03$ and that $-y_v$ will be considerably smaller than $0 \cdot 2$. The relative-density factor $\mu$ on an all-wing design should not exceed 40. Information at present available on this type of aircraft indicates that $i_A$ and $i_C$ will be in the region of $0 \cdot 09$ to $0 \cdot 12$ and that their difference will probably be small. With these facts in mind the following ranges have been investigated : $\mu n_v = 0$ to $1 \cdot 4$, $-n_r = 0$ to $0 \cdot 03$, $-y_v = 0$ to $0 \cdot 2$ for several different combinations of inertias.

*R.A.E. Report No. Aero. 1826 received 30th July, 1943.

2. *Notation.*—The notation is based on that of R. & M. 1801[3] from which many of the following definitions are taken. Many revisions are due to Dr. Mitchell.[4]

The $x$-axis is taken into the direction of the relative wind in the undisturbed condition and in all this work has been assumed to be horizontal. The $y$-axis is along the wing, positive in the starboard direction. The $z$-axis is then perpendicular to the $x$- and $y$-axes and is positive downwards. These axes remain fixed in the body in the disturbed motion.

The forces and velocities along these axes and the couples and angular velocities about them are defined below :—

| Axis | Force in direction of axis | Couple about axis | Velocity in direction of axis | Angular velocity about axis |
|---|---|---|---|---|
| $Ox$ | $X$ | $L$ | $V + u$ | $p$ |
| $Oy$ | $Y$ | $M$ | $v$ | $q$ |
| $Oz$ | $Z$ | $N$ | $w$ | $r$ |

These may be expressed in the following non-dimensional form :—

$$C_y = \frac{Y}{\frac{1}{2}\rho V^2 S}, \qquad C_l = \frac{L}{\rho V^2 Ss}, \qquad C_n = \frac{N}{\rho V^2 Ss},$$

$$\hat{v} = \frac{v}{V}, \qquad \hat{p} = \frac{\mu p s}{V}, \qquad \hat{r} = \frac{\mu r s}{V},$$

where $S$ is the gross wing area and $s$ is the semi-span and $\mu$ is the relative density parameter $m/\rho Ss$.

The unit of time chosen is $\hat{t} = m/\rho SV = \mu s/V$. The symbol $d/d\tau$ denotes differentiation with respect to this unit of time.

The moments of inertia about the axes $Ox$ and $Oz$ are denoted by $A$ and $C$ respectively and these are expressed in coefficient form as follows :—

$$i_A = \frac{A}{ms^2}, \qquad i_C = \frac{C}{ms^2}.$$

The product of inertia about the axes $Ox$ $Oz$ is denoted by $E$ and the dimensionless coefficient by $i_E = - E/ms^2$. The ratios $E/A$ and $E/C$ are denoted by $\varepsilon_A$ and $\varepsilon_C$ respectively.

The aerodynamic derivatives can be expressed as

$$y_v = \frac{1}{2}\frac{\partial C_y}{\partial \beta}, \qquad l_v = \frac{\partial C_l}{\partial \beta}, \qquad n_v = \frac{\partial C_n}{\partial \beta},$$

$$l_p = \frac{\partial C_l}{\partial (ps/V)}, \qquad n_p = \frac{\partial C_n}{\partial (ps/V)},$$

$$l_r = \frac{\partial C_l}{\partial (rs/V)}, \qquad n_r = \frac{\partial C_n}{\partial (rs/V)}.$$

In this notation $y_v$, $l_v$, $l_p$, $n_p$, $n_r$, are usually negative and $n_v$ and $l_r$ are usually positive. In order to facilitate numerical calculation it is convenient to write

$$\bar{y}_v = -y_v\,, \qquad \mathscr{L} = -\frac{\mu l_v}{i_A}\,, \qquad \mathscr{N} = \frac{\mu n_v}{i_C}\,,$$
$$l_1 = -\frac{l_p}{i_A}\,, \qquad n_1 = -\frac{n_p}{i_C}\,,$$
$$l_2 = \frac{l_r}{i_A}\,, \qquad n_2 = -\frac{n_r}{i_C}\,.$$

With this notation the equations of motion under no external forces in horizontal flight become

$$\left.\begin{aligned}
&\left(\frac{d}{d\tau}+\bar{y}_v\right)\hat{v} && && +\hat{r} \quad -k\phi = 0\,,\\
&\mathscr{L}\,\hat{v} && +\left(\frac{d}{d\tau}+l_1\right)\hat{p} && +\left(\varepsilon_A\frac{d}{d\tau}-l_2\right)\hat{r} \quad = 0\,,\\
&-\mathscr{N}\,\hat{v} && +\left(\varepsilon_C\frac{d}{d\tau}+n_1\right)\hat{p} && +\left(\frac{d}{d\tau}+n_2\right)\hat{r} \quad = 0\,,\\
& && -\hat{p} && +\frac{d}{d\tau}\phi = 0\,,
\end{aligned}\right\}$$

and the stability equation becomes

$$A\lambda^4 + B\lambda^3 + C\lambda^2 + \mathrm{D}\lambda + E = 0\,,$$

where
$$\begin{aligned}
A &= 1 - \varepsilon_A\,\varepsilon_C\,,\\
B &= l_1 + n_2 + \varepsilon_C l_2 - \varepsilon_A n_1 + y\ \ (1 - \varepsilon_A\varepsilon_C)\,,\\
C &= (l_1 n_2 + l_2 n_1) + \bar{y}_v\,(l_1 + n_2 + \varepsilon_C l_2 - \varepsilon_A n_1) + \varepsilon_C\mathscr{L} + \mathscr{N}\,,\\
D &= \bar{y}_v\,(l_1 n_2 + l_2 n_1) + (\mathscr{L} n_1 + \mathscr{N} l_1) + k\,(\mathscr{L} + \mathscr{N}\varepsilon_A)\,,\\
E &= k\,(\mathscr{L} n_2 - \mathscr{N} l_2)\,.
\end{aligned}$$

All the stability diagrams and curves of constant damping have been plotted with $\mu n_v$ and $-\mu l_v$ as co-ordinates and it is convenient to calculate them first in terms of $\mathscr{N}$ and $\mathscr{L}$; for this reason the coefficients which are dependent on these quantities are conveniently written

$$\begin{aligned}
C &= C_1 + C_2\mathscr{L} + C_3\mathscr{N}\,,\\
D &= D_1 + D_2\mathscr{L} + D_3\mathscr{N}\,,\\
E &= \qquad E_2\mathscr{L} - E_3\mathscr{N}\,,
\end{aligned}$$

where

$$\begin{aligned}
A &= 1 - \varepsilon_A\,\varepsilon_C\,,\\
B &= (l_1 + n_2 + \varepsilon_C l_2 - \varepsilon_A n_1) + \bar{y}_v\,(1 - \varepsilon_A\,\varepsilon_C)\,,\\
C_1 &= (l_1 n_2 + l_2 n_1) + \bar{y}_v\,(l_1 + n_2 + \varepsilon_C l_2 - \varepsilon_A n_1)\,, \quad C_2 = \varepsilon_C\,,\ C_3 = 1\,,\\
D_1 &= \bar{y}_v\,(l_1 n_2 + l_2 n_1)\,, \quad D_2 = (n_1 + k)\,, \quad D_3 = (l_1 + k\varepsilon_A)\,,\\
E_2 &= k n_2\,, \quad E_3 = k l_2\,.
\end{aligned}$$

3. *Stability Boundaries.*—It has been shown by Routh[5] that the conditions for stability are that $E$ shall be positive and the expression $D(BC - AD) - B^2E$ is positive. If $E$ is negative, the motion will contain a divergence, and if $D(BC - AD) - B^2E$ is negative the motion will contain a divergent oscillation.

We therefore calculate the points at which $E$ and $D(BC - AD) - B^2E$ change sign.

3.1. *Method of Calculation.*—The $E = 0$ boundary is with the assumptions of this work a straight line through the origin and is easily plotted from its equation

$$E_2\mathscr{L} - E_3\mathscr{N} = 0 .$$

The following method of calculating the oscillation boundary is due to Dr. Mitchell.

The oscillation boundary is given by

$$D - \frac{BE}{C - AD/B} = 0 ,$$

*i.e.*
$$D\,(BC - AD) - B^2E \equiv R = 0 .$$

Let
$$R' = BC - AD ;$$

then
$$R' = R_1' - R_2'\mathscr{L} + R_3'\mathscr{N} ,$$

where
$$R_1' = BC_1 - AD_1 , \quad R_2' = AD_2 - BC_2 , \quad R_3' = BC_3 - AD_3 .$$

Let the values of $\mathscr{L}$ on $D = 0$, $R' = 0$, $E = 0$ and $R = 0$, corresponding to the value $\mathscr{N}_1$ be denoted by $-\mathscr{L}_D$, $\mathscr{L}_{R'}$, $\mathscr{L}_E$ and $\mathscr{L}_1$ respectively ; then

$$E\,(\mathscr{L}_1\mathscr{N}_1) = E_2\mathscr{L}_1 - E_3\mathscr{N}_1 ,$$

$$E(\mathscr{L}_E\mathscr{N}_1) = E_2\mathscr{L}_E - E_3\mathscr{N}_1 = 0 ,$$

so that
$$E(\mathscr{L}_1\mathscr{N}_1) = E_2(\mathscr{L}_1 - \mathscr{L}_E) .$$

Similarly
$$D(\mathscr{L}_1\mathscr{N}_1) = D_2(\mathscr{L}_1 + \mathscr{L}_D) ,$$

$$R'(\mathscr{L}_1\mathscr{N}_1) = R_2'(\mathscr{L}_{R'} - \mathscr{L}_1) ;$$

therefore
$$R(\mathscr{L}_1\mathscr{N}_1) = D(\mathscr{L}_1\mathscr{N}_1)\; R'(\mathscr{L}_1\mathscr{N}_1) - B^2E(\mathscr{L}_1\mathscr{N}_1)$$

$$= D_2(\mathscr{L}_1 + \mathscr{L}_D)\; R_2'(\mathscr{L}_{R'} - \mathscr{L}_1) - B^2E_2(\mathscr{L}_1 - \mathscr{L}_E) ,$$

*i.e.*
$$\mathscr{L}_1^{\,2} - \left\{\mathscr{L}_{R'} - \mathscr{L}_D - \frac{B^2E_2}{D_2R_2'}\right\}\mathscr{L}_1 - \left\{\mathscr{L}_{R'}\,\mathscr{L}_D + \frac{B^2E_2}{D_2R_2'}\,\mathscr{L}_E\right\} = 0 .$$

The Method employed was to calculate $A$, B, $C_1$, $C_2$, etc. $R_1'$, $R_2'$, $R_3'$, $B^2E_2/D_2R_2'$, and hence obtain at the required values of $\mathscr{N}$; $\mathscr{L}_E$, $\mathscr{L}_{R'}$ , and $\mathscr{L}_D$ and hence calculate

$$\Phi = \mathscr{L}_{R'} - \mathscr{L}_D - \frac{B^2E_2}{D_2R_2'}, \quad \Psi = \mathscr{L}_{R'}\,\mathscr{L}_D + \frac{B^2E_2}{D_2R_2'}\,\mathscr{L}_E$$

and obtain two values of $\mathscr{L}_1$ by solution of the quadratic equation.

3.2. *Values of Derivatives and other Parameters.*—It is considered that derivatives $l_p$, $l_r$, $n_p$, which are principally due to the wing, should be of the same order as for a conventional design.* For most of the present work therefore, the values assumed in Priestley's investigation (R. & M. 1989, Pt. I[1]) have been used. These are

| | At $C_L = 0\cdot 1$ | At $C_L = 1\cdot 0$ |
|---|---|---|
| $l_p$ .. .. | $-0\cdot 45$ | $-0\cdot 40$ |
| $l_r$ .. .. | $0\cdot 02$ | $0\cdot 235$ |
| $n_p$ .. .. | $-0\cdot 03$ | $-0\cdot 05$ |

For $C_L = 0\cdot 1$ the product-of-inertia term $i_E$ was taken to be zero and for $C_L = 1\cdot 0$, $i_E$ was assumed to be $-(i_C - i_A)\sin\varepsilon\cos\varepsilon$, and $\varepsilon$ was assumed to be $-10$ deg.

Boundaries where $R = 0$ and $E = 0$ have been calculated for the extreme values $y_v = 0$ and $y_v = -0\cdot 2$ with each of the values $n_r = 0$ and $n_r = -0\cdot 03$ for the following pairs of inertias :— $i_A = 0\cdot 05$, $i_C = 0\cdot 08$ ; $i_A = 0\cdot 09$, $i_C = 0\cdot 09$ ; $i_A = 0\cdot 09$, $i_C = 0\cdot 12$ ; $i_A = 0\cdot 12$, $i_C = 0\cdot 12$. All these calculations have been made both for $C_L = 0\cdot 1$ and $C_L = 1\cdot 0$. In order to examine the variation of the boundaries with $y_v$ and $n_r$ more fully, boundaries have been calculated for all possible combinations of the following values of $y_v$ and $n_r$ :—

$$\left.\begin{array}{lllll} y_v = 0\,, & -0\cdot 05\,, & -0\cdot 10\,, & -0\cdot 15\,, & -0\cdot 20\,, \\ n_r = 0\,, & -0\cdot 01\,, & -0\cdot 02\,, & -0\cdot 03\,, & \end{array}\right\}$$

for $\quad i_A = 0\cdot 12\,, \qquad i_C = 0\cdot 12\,, \qquad$ at $C_L = 0\cdot 1$ .

Boundaries have also been calculated to show the effect of varying $l_p$, $l_r$, $n_p$ from the standard values given above in the case $y_v = -0\cdot 05$, $n_r = -0\cdot 01$, $i_A = 0\cdot 12$, $i_C = 0\cdot 12$.

The numerical field surveyed is summarised in Table 2.

3.3. *Variation of Stability Boundaries with the Parameters.*—3.31. *Variation with $y_v$ and $n_r$.*—The "spiral" boundaries have the equation $n_2\mathscr{L} - l_2\mathscr{N} = 0$ (for stability the left-hand side must be positive) or multiplying by $i_A \,.\, i_C$

$$(-\mu l_v)\,(-n_r) - (\mu n_v)\,l_r = 0\,,$$

so that the $E$ boundary is a straight line through the origin with slope $l_r/-n_r$.

The oscillation boundaries are displaced upwards with increase of either $-y_v$ or $-n_r$. The rate of displacement upwards is greater at $C_L = 0\cdot 1$ than at $C_L = 1\cdot 0$ (Figs. 2 and 11). In the one case in which a larger number of these parameters was considered ($i_A = 0\cdot 12$, $i_C = 0\cdot 12$, $C_L = 0\cdot 1$) the variation with $y_v$ and $n_r$ was found to be very nearly linear (Figs. 5–9) so that further detailed calculations of this type were considered unnecessary.

3.32. *Variation with $C_L$.*—It has been shown elsewhere that for the values of the parameters usual in conventional designs, the $R = 0$ boundaries are displaced downwards with increase of $C_L$. In the range considered here the $R = 0$ boundaries are displaced downwards with increase of $C_L$ at the higher values of $y_v$ and $n_r$, but the direction of displacement is reversed at lower values of these parameters. At low values of $C_L$ and very low values of $y_v$ and $n_r$ the stable region becomes very small.

*There is most likelihood of variation in $l_r$ and $n_p$ since these parameters depend on the moment of inertia of the lift distribution about the axis of the aircraft. Tailless designs incorporate a fairly large washout and at low $C_L$ the lift at the tip may be negative, thus substantially reducing both $l_r$ and $n_p$. The effect of variation of these parameters is dealt with in §3.35 and Figs. 14–19. The effect of changes in $l_p$ is not large, but overestimation of the numerical value of $n_p$ may make the conclusions of this report rather on the pessimistic side.

The " spiral " boundary is a straight line through the origin with slope $l_r/-n_r$, *i.e.* the slope is roughly proportional to $C_L$.

3.33. *Variation with* $\mu$.—The stability boundaries of this report are plotted with $\mu n_v$ and $-\mu l_v$ as co-ordinates and in this way are made independent of $\mu$. It is obvious however that if they are plotted in the usual way against $n_v$ and $-l_v$ the oscillation boundary will be displaced downwards with increase of $\mu$.

3.34. *Variation with Inertia.*—The few variations of inertia coefficients that have been considered are not sufficient to give any clear indication of the manner in which the oscillation boundaries vary with inertia. They do, however, serve to illustrate the general result that the region of stability tends to decrease when $i_A$ and $i_C$ increase together.

3.35. *Variation with* $l_p$, $l_r$ and $n_p$.—Calculations have been made to investigate the effect on the $R = 0$ boundaries if $l_p$, $l_r$ and $n_p$ deviate from the standard values used in the remainder of the work.

An increase of $-l_p$ causes a fairly large increase of the stable region in the case considered both when $C_L = 0\cdot 1$ and when $C_L = 1\cdot 0$. This is shown in Figs. 14 and 17. The variation of $l_r$ seems unimportant at $C_L = 0\cdot 1$, but increases in importance when $C_L = 1\cdot 0$; in both cases a decrease of $l_r$ causes the $R = 0$ boundary to be displaced downwards (Figs. 15 and 18). Changes in $n_p$ seem to have a small effect at $C_L = 1\cdot 0$, but a much greater effect at $C_L = 0\cdot 1$, the boundary being displaced ***downwards*** with increase of $-n_p$ (Figs. 16 and 19).

The $E = 0$ boundary is independent of $l_p$ and $n_p$ and has a slope proportional to $-l_r$.

4. *Curves of Constant Damping.*—Curves of constant damping of the oscillatory and of the spiral motions have been calculated in a few cases to indicate the gradient of damping across the boundaries. The inertias $i_A = 0\cdot 12$, $i_C = 0\cdot 12$ have been used and the curves have been calculated for the pairs of values $y_v = 0$, $n_r = 0$; $y_v = -0\cdot 05$, $n_r = -0\cdot 01$; $y_v = -0\cdot 10$, $n_r = -0\cdot 02$.

4.1. *Method of Calculation.*—The curves of constant damping have been calculated by the method described by Brown (R. & M. 1905[6]).

If $r_l \pm is_l$ are two roots of

$$A\lambda^4 + B\lambda^3 + C\lambda^2 + D\lambda + E = 0\,,$$

then
$$As_l^4 - if_3(r_l)\, s_l^3 - f_2(r_l)\, s_l^2 + if_1(r_l)\, s_l + f(r_l) = 0\,,$$

where
$$f(r_l) = Ar_l^4 + Br_l^3 + Cr_l^2 + Dr_l + E\,,$$

$$f_1(r_l) = 4Ar_l^3 + 3Br_l^2 + 2Cr_l + D\,,$$

$$f_2(r_l) = 6Ar_l^2 + 3Br_l + C\,,$$

$$f_3(r_l) = 4Ar_l + B\,,$$

and equating real and imaginary parts

$$\left.\begin{aligned} As_l^4 - f_2(r_l)s_l^2 + f(r_l) &= 0\,, \\ f_3(r_l)s_l^2 - f_1(r_l) &= 0\,. \end{aligned}\right\}$$

Now $f(r_l)$ can be written

$$f(r_l) = f_{01}(r_l) + f_{02}(r_l)\,\mathscr{L} + f_{03}(r_l)\mathscr{N}\,,$$

where
$$f_{01}(r_l) = Ar_l^4 + Br_l^3 + C_1r_l^2 + D_1r_l\,,$$
$$f_{02}(r_l) = C_2r_l^2 + D_2r_l + E_2\,,$$
$$f_{03}(r_l) = C_3r_l^2 + D_3r_l - E_3\,,$$

and similarly for $f_1, f_2, f_3$.

Now if we write
$$a_1 = As_l^4 - f_{21}(r_l)s_l^2 + f_{01}(r_l)\,,$$
$$b_1 = f_{02}(r_l) - f_{22}(r_l)s_l^2\,,$$
$$c_1 = f_{03}(r_l) - f_{23}(r_l)s_l^2\,,$$
$$a_2 = f_{11}(r_l) - f_{31}(r_l)s_l^2\,,$$
$$b_2 = f_{12}(r_l)\,,$$
$$c_2 = f_{13}(r_l)\,,$$

the equations become
$$\left.\begin{aligned} a_1 + b_1\mathscr{L} + c_1\mathscr{N} = 0\,,\\ a_2 + b_2\mathscr{L} + c_2\mathscr{N} = 0\,,\end{aligned}\right\}$$

which can be solved for $\mathscr{L}$ and $\mathscr{N}$.

4.2. *Results of Period and Damping Calculations.*—The curves of constant damping show that there is little variation of the gradient of damping across the R = 0 boundary with change of $y_v$ and $n_r$.

When $C_L = 0 \cdot 1$ the gradient of damping across the boundary $E = 0$ is very small so that no appreciable change in the spiral motion is likely to occur within the practical region of $l_v$ and $n_v$.

5. *Aircraft with Fins.*—The present work has been undertaken mainly to investigate the characteristics of a pure flying wing with no fins. If there are fins there will be a linear relation between $n_v$ and $n_r$ due to the contribution of the fin. The value of $l_v$ to give $R = 0$ or $E = 0$ may be interpolated at any $n_v$ and $n_r$ from the figures given and a stability diagram may be constructed. The stability diagram would in this case have an $R$ boundary of degree 4 and an E boundary of degree 2 as in the case of conventional aircraft. The $R$ and $E$ boundaries will in general have one more intersection in the region of positive $n_v$ and negative $l_v$ and there will be two completely stable regions, one for small values of $l_v$ and $n_v$ and one for larger values of both parameters. The constant $b$ in the relation $n_r = a + b\ n_v$ will for tailless aircraft be much smaller than for conventional aircraft (since the fin arm will be smaller), hence the two intersections of $R = 0$ and $E = 0$ will be farther apart and the region of large $l_v$ and $n_v$ may not be accessible.

6. *Numerical Comparison with Conventional Aircraft.*—Very few data are at present available on the probable values of the derivatives for all-wing aircraft. Recent wind-tunnel tests on a swept-back wing have shown that $n_v$ may vary from about $0 \cdot 005$ at low incidences to $0 \cdot 01$ at high incidences; $l_v$ can be varied for any design by a change of dihedral, but there will be a considerable change in $l_v$ with $C_L$ due to the large sweepback which is necessary in tailless aircraft to solve the problems of longitudinal stability and trim. In these recent tests $l_v$ varied from $-0 \cdot 04$ to $-0 \cdot 11$. The same tests indicate that $y_v$ will probably be in the region of $-0 \cdot 01$.

During systematic tests of rolling moment due to sideslip[7] yawing moments were measured on a few swept-back and swept-forward wings. These results indicate that there is no great change of $n_v$ due to sweepback at zero incidence, but that there is a greater increase of $n_v$ with incidence on those wings with greater sweepback.

There is even less information on the value of $n_r$ and we can only follow Reference 1 and assume that $n_r$ for a wing alone will be of the order 0 to $-0 \cdot 01$. For the remainder of the derivatives it is assumed that the values will approximate to those given in R. & M. 1989, Pt. I[1] and § 3.2 of this report.*

It has been shown[8] that from constructional and performance considerations comparable conventional and all-wing designs are given by the following Table :—

| | | Conventional | All-wing |
|---|---|---|---|
| Weight (lb.) | $W$ | 60,000 | 60,000 |
| Span (ft.) | $b$ | 100 | 100 |
| Wing loading (lb./sq. ft.) | | 50 | 35 |

The change of loading from conventional to an all-wing design will largely consist of a removal of load in the rear fuselage and an increase of load in the wing tips. This will give little variation in the moment of inertia $C$, but a considerable increase in $A$ so that the difference $C - A$ becomes small. The values assumed for the two cases are therefore, for the conventional aircraft $i_A = 0 \cdot 0625$, $i_C = 0 \cdot 1225$ and for the tailless $i_A = 0 \cdot 12$, $i_C = 0 \cdot 12$.

We can now summarise the important parameters for the two types of aircraft.

| | | | Conventional | All-wing |
|---|---|---|---|---|
| Weight (lb.) | | $W$ | 60,000 | 60,000 |
| Span (ft.) | | $b$ | 100 | 100 |
| Wing loading (lb./sq. ft.) | | $w$ | 50 | 35 |
| Inertia coefficients | | $i_A$ | $0 \cdot 0625$ | $0 \cdot 12$ |
| | | $i_C$ | $0 \cdot 1225$ | $0 \cdot 12$ |
| | | $y_v$ | $-0 \cdot 2$ | 0 and $-0 \cdot 05$ |
| Relative density parameter $\mu$ | | at sea level | 13 | 9 |
| | | at 40,000 ft. | 52 | 36 |
| Unit of time $\hat{t}$ | $C_L = 0 \cdot 1$ | at sea level | $1 \cdot 42$ | $1 \cdot 19$ |
| | | at 40,000 ft. | $2 \cdot 85$ | $2 \cdot 38$ |
| | $C_L = 1 \cdot 0$ | at sea level | $4 \cdot 50$ | $3 \cdot 77$ |
| | | at 40,000 ft. | $9 \cdot 01$ | $7 \cdot 54$ |

For comparison, curves of constant damping have been drawn for the conventional aircraft outlined above at $C_L = 0 \cdot 1$. As a rough comparison with the curves for the tailless aircraft at $C_L = 1 \cdot 0$ the curves of R. & M. 1989 Pt. II[2] may be used. These curves are not strictly comparable since the curves of this report are for level flight and those at $C_L = 1 \cdot 0$ in R. & M. 1989, Pt. II[2] are for $\tan \theta_0 = -0 \cdot 1$.

To obtain a numerical comparison we shall consider the values for the conventional aircraft :—

(a) $n_v = 0 \cdot 02$ , $l_v = -0 \cdot 02$ ,

(b) $n_v = 0 \cdot 02$ , $l_v = -0 \cdot 10$ ,

(c) $n_v = 0 \cdot 10$ , $l_v = -0 \cdot 02$ ,

(d) $n_v = 0 \cdot 10$ , $l_v = -0 \cdot 10$ ,

at $C_L = 0 \cdot 1$ and $C_L = 1 \cdot 0$.

*But *see* footnote to §3.2.

For the tailless aircraft

$$\left.\begin{array}{llll}(\alpha)\ n_r = 0\,, & y_v = 0\,, & n_v = 0\,, & l_v = -0\cdot01\,, \\ (\beta)\ n_r = 0\,, & y_v = 0\,, & n_v = 0\,, & l_v = -0\cdot05\,, \\ (\gamma)\ n_r = -0\cdot01\,, & y_v = -0\cdot05\,, & n_v = 0\cdot01\,, & l_v = -0\cdot01\,, \\ (\delta)\ n_r = -0\cdot01\,, & y_v = -0\cdot05\,, & n_v = 0\cdot01\,, & l_v = -0\cdot05\,, \end{array}\right\} C_L = 0\cdot1\,,$$

$$\left.\begin{array}{llll}(\varepsilon)\ n_r = 0\,, & y_v = 0\,, & n_v = 0\cdot01\,, & l_v = -0\cdot01\,, \\ (\zeta)\ n_r = 0\,, & y_v = 0\,, & n_v = 0\cdot01\,, & l_v = -0\cdot05\,, \\ (\eta)\ n_r = -0\cdot01\,, & y_v = -0\cdot05\,, & n_v = 0\cdot02\,, & l_v = -0\cdot01\,, \\ (\theta)\ n_r = -0\cdot01\,, & y_v = -0\cdot05\,, & n_v = 0\cdot02\,, & l_v = -0\cdot05\,, \end{array}\right\} C_L = 1\cdot0\,.$$

The information at present available indicates that tailless designs will probably approximate more closely to cases $\alpha$, $\beta$, $\varepsilon$, $\zeta$, than to the others but will probably have parameters within the above ranges.

The dampings of the motions are compared in Table 1.

It will be seen that a tailless aircraft is almost certain to be spirally unstable. At low $C_L$ the rate of divergence will be slow and at high $C_L$ the rate of divergence is of the same order as for a conventional aircraft.

The oscillation may be unstable in all conditions and in no case will the damping be large. The lateral oscillations may be less troublesome on a tailless aircraft because of the rather longer period.

In view of the uncertainty of the derivatives it is difficult to form any definite conclusions about the stability of tailless aircraft. These calculations show that the achievement of stability may be difficult. This difficulty is due to the small values of $n_v$ and $n_r$ and at present there is no information on the size of $n_r$. It will be seen from the stability diagrams, Figs. 5–9, that this derivative is of considerable importance and until more information becomes available it is difficult to obtain with any accuracy an estimate of the stability characteristics of tailless designs.

7. *Conclusions*.—The conclusions of this work are compared with the corresponding conclusions for a conventional design (from R. & M. 1989, Pt. I[1]).

| Conventional aircraft | Tailless aircraft |
|---|---|
| (1) At high speed, spiral instability is very unlikely to be met. | At high speed, spiral instability is likely to occur unless $-l_v$ is large. |
| (2) The oscillation will usually be stable at high speed provided $n_v > 0$. | The oscillation is likely to be unstable* at high speed unless $-l_v$ is small or $-n_v$ or $-y_v$ have the larger values considered. |
| (3) At low speed, spiral instability is almost certain. | At low speed, spiral instability is even more likely to occur than on a conventional aircraft. |
| (4) At low speed, the oscillation will usually be unstable except for low $l_v$ or $n_v$. | Oscillatory instability is more likely to occur at low speed than at high for the larger values of $-n_r$ and $-y_v$ considered. For the smaller values of $-y_v$ and $-n_r$ the oscillation is more likely to be unstable at high speed than at low. A low value of $l_v$ will be required for stability. |

*But *see* footnote to §3.2.

## LIST OF SYMBOLS

| | |
|---|---|
| $A$ | Moment of inertia of aircraft in roll. |
| $A, B, C, D, E$ | Coefficients of stability quartic $f(\lambda)$. |
| $C$ | Moment of inertia of aircraft in yaw. |
| $C_1, D_1$ | Terms independent of $\mathscr{L}$ and $\mathscr{N}$ in coefficients $C$ and $D$. |
| $C_2, D_2, E_2$ | Coefficients of $\mathscr{L}$ in $C$, $D$ and $E$. |
| $C_3, D_3, -E_3$ | Coefficients of $\mathscr{N}$ in $C$, $D$ and $E$. |
| $E$ | Product of inertia of aircraft about the axes of roll and yaw. |
| $f(\lambda)$ | The stability quartic $A\lambda^4 + B\lambda^3 + C\lambda^2 + D\lambda + E$. |
| $f_1, f_2, f_3, f_4$ | The coefficients of the Taylor expansion of $f$. |
| $f_{01}, f_{11}, f_{21}$, *etc.* | The terms of $f, f_1, f_2$, *etc.* independent of $\mathscr{L}$ and $\mathscr{N}$. |
| $f_{02}, f_{12}$, *etc.* | The coefficients of $\mathscr{L}$ in $f, f_1$, *etc.* |
| $f_{03}, f_{13}$, *etc.* | The coefficients of $\mathscr{N}$ in $f, f_1$, *etc.* |
| $i_A, i_C$ | Inertia coefficients in roll and yaw $i_A = A/ms^2$. |
| $i_E$ | Product of inertia coefficient about the rolling and yawing axes. $i_E = -E/ms^2$. |
| $k$ | $\frac{1}{2}C_L$. |
| $\mathscr{L}$ | $-\mu l_v/i_A$. |
| $\mathscr{L}_D, \mathscr{L}_{R'}, \mathscr{L}_E, \mathscr{L}_1$ | Values of $\mathscr{L}$ corresponding to $\mathscr{N} = \mathscr{N}_1$ on $D = 0$, $R' = 0$, $E = 0$ and $R = 0$ respectively. |
| $l_v$ | Coefficient of rolling moment due to sideslip, $\partial C_l/\partial\beta$. |
| $l_p$ | Coefficient of rolling moment due to rolling, $\partial C_l/\partial(ps/V)$. |
| $l_r$ | Coefficient of rolling moment due to yawing $\partial C_l/\partial(rs/V)$. |
| $l_1$ | $-l_p/i_A$. |
| $l_2$ | $l_r/i_A$. |
| $\mathscr{N}$ | $\mu n_v/i_C$ |
| $n_v$ | Coefficient of yawing moment due to sideslip, $\partial C_n/\partial\beta$. |
| $n_p$ | Coefficient of yawing moment due to rolling, $\partial C_n/\partial(ps/V)$. |
| $n_r$ | Coefficient of yawing moment due to yawing, $\partial C_n/\partial(rs/V)$. |
| $n_1$ | $-n_p/i_C$. |
| $n_2$ | $-n_r/i_C$. |
| $\hat{p}$ | Dimensionless coefficient of rolling velocity, $\mu ps/V$. |
| $R$ | Routh's discriminant, $D(BC - AD) - B^2E$. |
| $R'$ | Test function $(BC - AD)$. |
| $R_1'$ | Term of $R'$ independent of $\mathscr{L}$ and $\mathscr{N}$. |
| $R_2', R_3'$ | Coefficients of $\mathscr{L}$ and $\mathscr{N}$ in $R'$. |
| $\hat{r}$ | Dimensionless coefficient of yawing velocity, $\mu rs/V$ |

## LIST OF SYMBOLS—*contd.*

| | |
|---|---|
| $r$ | Damping coefficient of lateral oscillation. |
| $r_s$ | Damping coefficient of " spiral " motion. |
| $s$ | Semispan of aircraft, $\frac{1}{2}b$. |
| $s_l$ | Frequency coefficient of lateral oscillation. |
| $\hat{t}$ | Unit of time in dimensionless system, $m/\rho SV$. |
| $\hat{v}$ | Dimensionless coefficient of sideslip velocity. |
| $y_v$ | Coefficient of sideforce due to sideslip, $\frac{1}{2}\frac{\partial C_Y}{\partial \beta}$. |
| $\bar{y}_v$ | $-y_v$. |
| $\beta$ | Angle of sideslip ($\beta \simeq \hat{v}$ for small angles). |
| $\varepsilon$ | Angle between principal axis of inertia and $x$-axis. |
| $\varepsilon_A$ | $-E/A = i_E/i_A$. |
| $\varepsilon_C$ | $-E/C = i_E/i_C$. |
| $\lambda$ | Dummy variable of stability quartic. |
| $\mu$ | Aircraft relative density parameter, $m/\rho Ss$. |
| $\tau$ | Time in dimensionless units. |
| $\phi$ | Angle of bank. |
| $\Phi$, $\Psi$ | Coefficients in quadratic equation for $\mathscr{L}$ |

## REFERENCES


| No. | Author | Title, etc. |
|---|---|---|
| 1 | Priestley .. .. .. .. | A Further Investigation of Lateral Stability. R. & M. 1989, Part I. March, 1941. |
| 2 | Priestley .. .. .. .. | An Investigation of the Periods and Dampings of the Lateral (Asymmetric) Motions. R. & M. 1989, Part II. March, 1941. |
| 3 | Bryant and Gates .. .. .. | Nomenclature for Stability Coefficients. R. & M. 1801. October, 1937. |
| 4 | Mitchell .. .. .. .. | A Supplementary Notation for Theoretical Lateral Stability Calculations. R.A.E. Tech. Note No. Aero. 1183. A.R.C. 6797. May, 1943. (To be published). |
| 5 | Routh .. .. .. .. | The Advanced Part of a Treatise on the Dynamics of a System of Rigid Bodies. 6th Ed., Macmillan, 1930, pp. 221–226. |
| 6 | Brown .. .. .. .. | A Simple Method of Constructing Stability Diagrams. R. & M. 1905. October, 1942. |
| 7 | Irving, Batson and Warsap .. | Model Experiments on the Rolling Moment due to Sideslip of Tapered Wing Monoplanes. R. & M. 2019. July, 1939. |
| 8 | Montagnon and Hallowes .. .. | Some Aspects of Large Aircraft Design. R.A.E. Report No. Aero. 1800. A.R.C. 6694. May, 1943. (To be published). |

## TABLE 1

*Numerical Comparison of a Tailless and a Conventional Aircraft*

$C_L = 0 \cdot 1$ Ground Level

| Case | | Conventional | | | | All-wing | | | |
|---|---|---|---|---|---|---|---|---|---|
| | | *a* | *b* | *c* | *d* | $\alpha$ | $\beta$ | $\gamma$ | $\delta$ |
| | $n_v$ | 0·02 | 0·02 | 0·10 | 0·10 | 0 | 0 | 0·01 | 0·01 |
| | $-l_v$ | 0·02 | 0·10 | 0·02 | 0·10 | 0·01 | 0·05 | 0·01 | 0·05 |
| Damping coefficient of oscillation | $r_l$ | −0·24 | −0·19 | −0·57 | −0·52 | +0·002 | +0·025 | −0·07 | −0·05 |
| Frequency coefficient of oscillation | $s_l$ | 1·5 | 1·7 | 3·4 | 3·4 | 0·25 | 0·25 | 0·7 | 0·8 |
| Damping coefficient of spiral motion | $r_s$ | −0·002 | −0·013 | −0·0003 | −0·01 | 0 | 0 | +0·001 | −0·001 |
| Oscillation: Period (secs.) | | 5·9 | 5·2 | 2·6 | 2·6 | 30 | 30 | 11 | 9 |
| Oscillation: Time to halve amplitude* (secs.) | | 4·1 | 5·2 | 1·7 | 1·9 | −400 | −30 | 12 | 16 |
| Spiral motion: Time to halve amplitude* (secs.) | | 500 | 76 | 3,000 | 100 | Neutral | | −800 | 800 |

$C_L = 0 \cdot 1$ 40,000 ft.

| Case | | Conventional | | | | All-wing | | | |
|---|---|---|---|---|---|---|---|---|---|
| | | *a* | *b* | *c* | *d* | $\alpha$ | $\beta$ | $\gamma$ | $\delta$ |
| | $n_v$ | 0·02 | 0·02 | 0·10 | 0·10 | 0 | 0 | 0·01 | 0·01 |
| | $-l_v$ | 0·02 | 0·10 | 0·02 | 0·10 | 0·01 | 0·05 | 0·01 | 0·05 |
| Damping coefficient of oscillation | $r_l$ | −0·21 | −0·05 | −0·55 | −0·44 | +0·028 | +0·10 | −0·045 | +0·005 |
| Frequency coefficient of oscillation | $s_l$ | 3·0 | 3·4 | 6·5 | 6·7 | 0·25 | 0·25 | 1·7 | 1·9 |
| Damping coefficient of spiral motion | $r_s$ | −0·002 | −0·013 | −0·0003 | −0·01 | 0 | 0 | +0·001 | −0·001 |
| Oscillation: Period (secs.) | | 5·9 | 5·3 | 2·8 | 2·7 | 60 | 60 | 8·8 | 7·9 |
| Oscillation: Time to halve amplitude* (secs.) | | 9·4 | 40 | 3·6 | 4·5 | −60 | −16 | 37 | −300 |
| Spiral motion: time to halve amplitude* (secs.) | | 1,000 | 150 | 6,500 | 200 | Neutral | | −1,600 | 1,600 |

*A negative sign indicates a divergence ; the figure given is then the time to double amplitude.

TABLE 1 (*cont.*)

$C_L = 1 \cdot 0$ Ground Level

| Case | | Conventional | | | | All-wing | | | |
|---|---|---|---|---|---|---|---|---|---|
| | | *a* | *b* | *c* | *d* | $\varepsilon$ | $\zeta$ | $\eta$ | $\theta$ |
| | $n_v$ | 0·02 | 0·02 | 0·10 | 0·10 | 0·01 | 0·01 | 0·02 | 0·02 |
| | $-l_v$ | 0·02 | 0·10 | 0·02 | 0·10 | 0·01 | 0·05 | 0·01 | 0·05 |
| Damping coefficient of oscillation | $r_l$ | −0·45 | −0·30 | −0·79 | −0·68 | −0·18 | −0·02 | −0·23 | −0·1 |
| Frequency coefficient of oscillation | $s_l$ | 1·7 | 2·2 | 3·4 | 3·7 | 1·1 | 1·3 | 1·4 | 1·6 |
| Damping coefficient of spiral motion | $r_s$ | +0·16 | 0 | +0·22 | +0·10 | +0·23 | +0·12 | +0·25 | +0·15 |
| Oscillation: Period (secs.) | | 17 | 13 | 8·3 | 7·6 | 22 | 18 | 17 | 15 |
| Oscillation: Time to halve amplitude* (secs.) | | 6·9 | 10·4 | 3·9 | 4·6 | 14 | 130 | 11 | 26 |
| Spiral motion: Time to halve amplitude* (secs.) | | −19 | Neutral | −14 | −31 | −11 | −22 | −10 | −17 |

$C_L = 1 \cdot 0$ 40,000 ft.

| Case | | Conventional | | | | All-wing | | | |
|---|---|---|---|---|---|---|---|---|---|
| | | *a* | *b* | *c* | *d* | $\varepsilon$ | $\zeta$ | $\eta$ | $\theta$ |
| | $n_v$ | 0·02 | 0·02 | 0·10 | 0·10 | 0·01 | 0·01 | 0·02 | 0·02 |
| | $-l_v$ | 0·02 | 0·10 | 0·02 | 0·10 | 0·01 | 0·05 | 0·01 | 0·05 |
| Damping coefficient of oscillation | $r_l$ | −0·40 | −0·14 | −0·75 | −0·58 | −0·08 | +0·3 | −0·13 | +0·18 |
| Frequency coefficient of oscillation | $s_l$ | 3·3 | 4·3 | 6·7 | 7·2 | 2·0 | 2·2 | 2·7 | 3·0 |
| Damping coefficient of spiral motion | $r_s$ | +0·17 | 0 | +0·23 | +0·10 | +0·23 | +0·12 | +0·25 | +0·15 |
| Oscillation: Period (secs.) | | 17 | 13 | 8·4 | 7·9 | 24 | 22 | 18 | 16 |
| Oscillation: Time to halve amplitude* (secs.) | | 16 | 45 | 8·3 | 10·8 | 65 | −17 | 40 | −29 |
| Spiral motion: Time to halve amplitude* (secs.) | | −37 | Neutral | −27 | −62 | −23 | −44 | −21 | −35 |

*A negative sign indicates a divergence ; the figure given is then the time to double amplitude.

# TABLE 2

*Key to Figures*

(1) Stability diagrams. Standard values of $l_p$, $l_r$, $n_p$

| $C_L$ | $-y_v$ | $-n_r$ | $i_A$ | $i_C$ | Fig. No. |
|---|---|---|---|---|---|
| 0·1 | 0 and 0·2 | 0 and 0·03 | 0·05 | 0·08 | 1 |
| | | | 0·09 | 0·09 | 2 |
| | | | 0·09 | 0·12 | 3 |
| | | | 0·12 | 0·12 | 4 |
| | 0 | 0, 0·01, 0·02, 0·03 | 0·12 | 0·12 | 5 |
| | 0·05 | | | | 6 |
| | 0·10 | | | | 7 |
| | 0·15 | | | | 8 |
| | 0·20 | | | | 9 |
| 1·0 | 0 and 0·2 | 0 and 0·03 | 0·05 | 0·08 | 10 |
| | | | 0·09 | 0·09 | 11 |
| | | | 0·09 | 0·12 | 12 |
| | | | 0·12 | 0·12 | 13 |

(2) Stability diagrams. Variation of $l_p$, $l_r$, $n_p$.

$$\left.\begin{array}{r} y_v = -0\cdot05,\ n_r = -0\cdot01 \\ i_A = 0\cdot12,\ i_C = 0\cdot12 \end{array}\right\} \begin{cases} C_L = 0\cdot1 \text{ Variation with } l_p \text{ Fig. 14} \\ C_L = 0\cdot1 \text{ Variation with } l_r \text{ Fig. 15} \\ C_L = 0\cdot1 \text{ Variation with } n_p \text{ Fig. 16} \\ C_L = 1\cdot0 \text{ Variation with } l_p \text{ Fig. 17} \\ C_L = 1\cdot0 \text{ Variation with } l_r \text{ Fig. 18} \\ C_L = 1\cdot0 \text{ Variation with } n_p \text{ Fig. 19} \end{cases}$$

(3) Curves of constant period and damping

$i_A = 0\cdot12 \qquad i_C = 0\cdot12$

| $C_L$ | $-y_v$ | $-n_r$ | Fig. No. |
|---|---|---|---|
| 0·1 | 0 | 0 | 20 |
| 0·1 | 0·05 | 0·01 | 21 |
| 0·1 | 0·10 | 0·02 | 22 |
| 1·0 | 0 | 0 | 23 |
| 1·0 | 0·05 | 0·01 | 24 |
| 1·0 | 0·10 | 0·02 | 25 |

(4) Curves of constant period and damping (conventional aircraft)

$i_A = 0\cdot0625 \qquad i_C = 0\cdot1225 \qquad C_L = 0\cdot1$

$\mu = 13$ Fig. 26
$\mu = 52$ Fig. 27

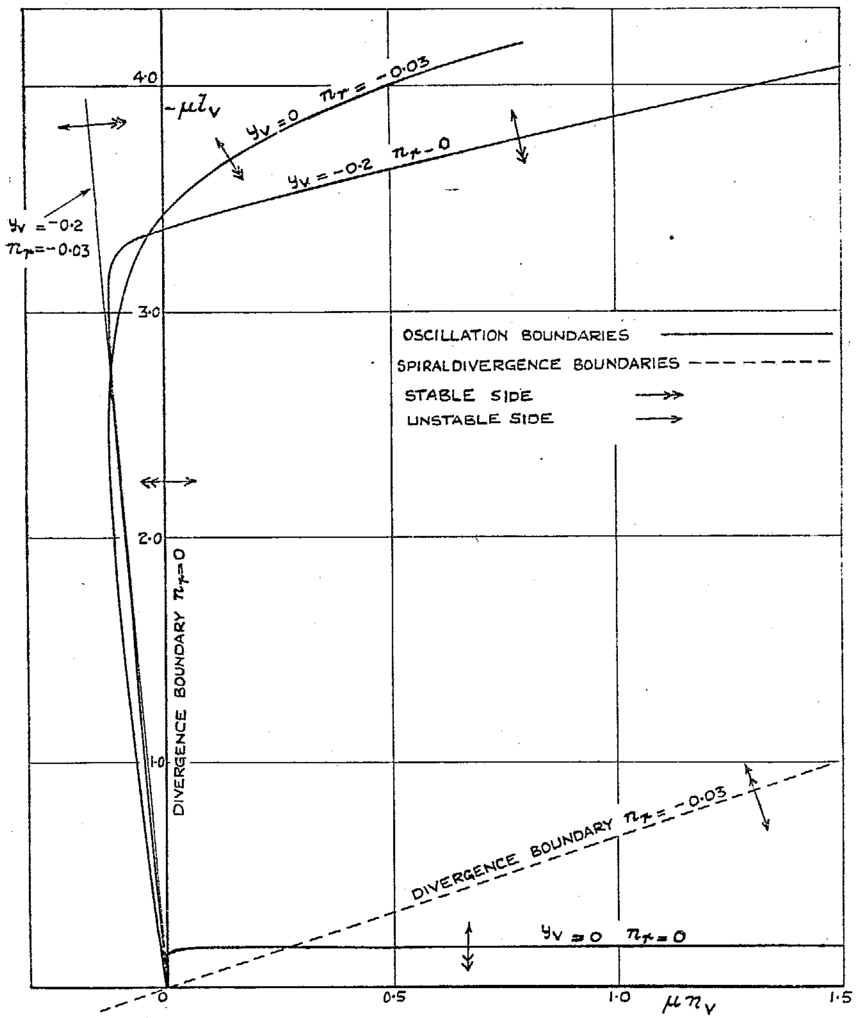


FIG. 1. Stability Boundaries $C_L = 0 \cdot 1$, $i_A = 0 \cdot 05$, $i_C = 0 \cdot 08$

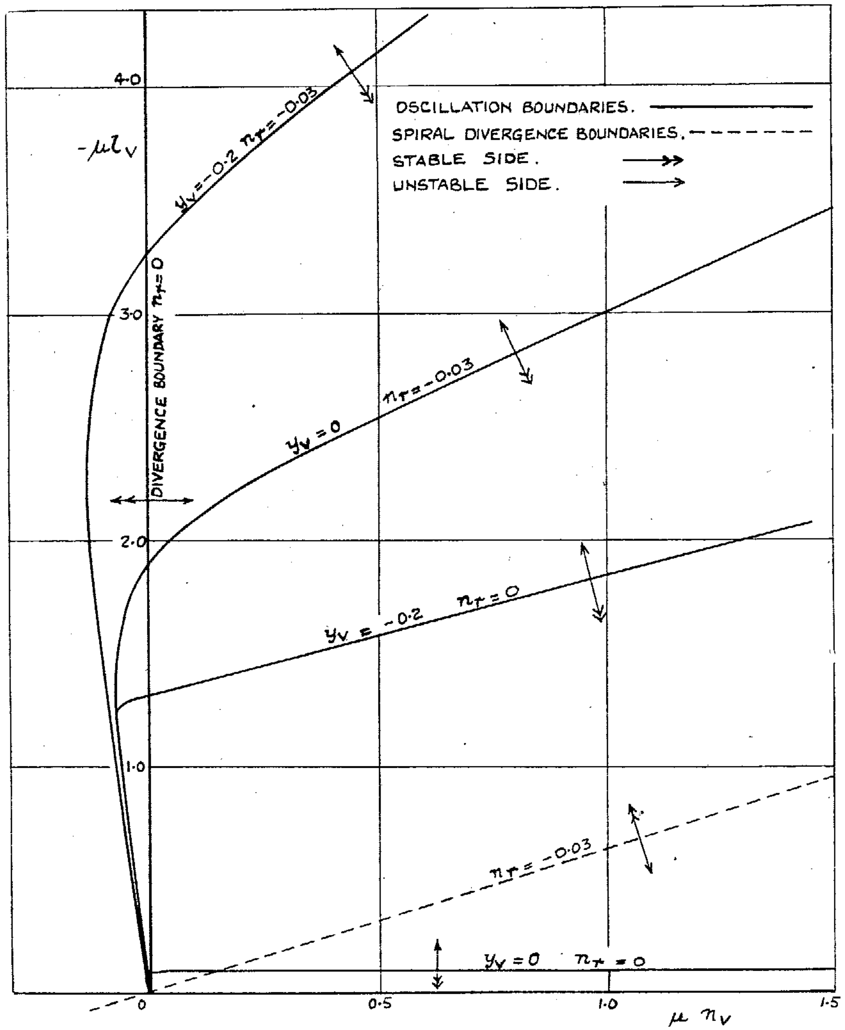


FIG. 2. Stability Boundaries $C_L = 0 \cdot 1$, $i_A = 0 \cdot 09$, $i_C = 0 \cdot 09$

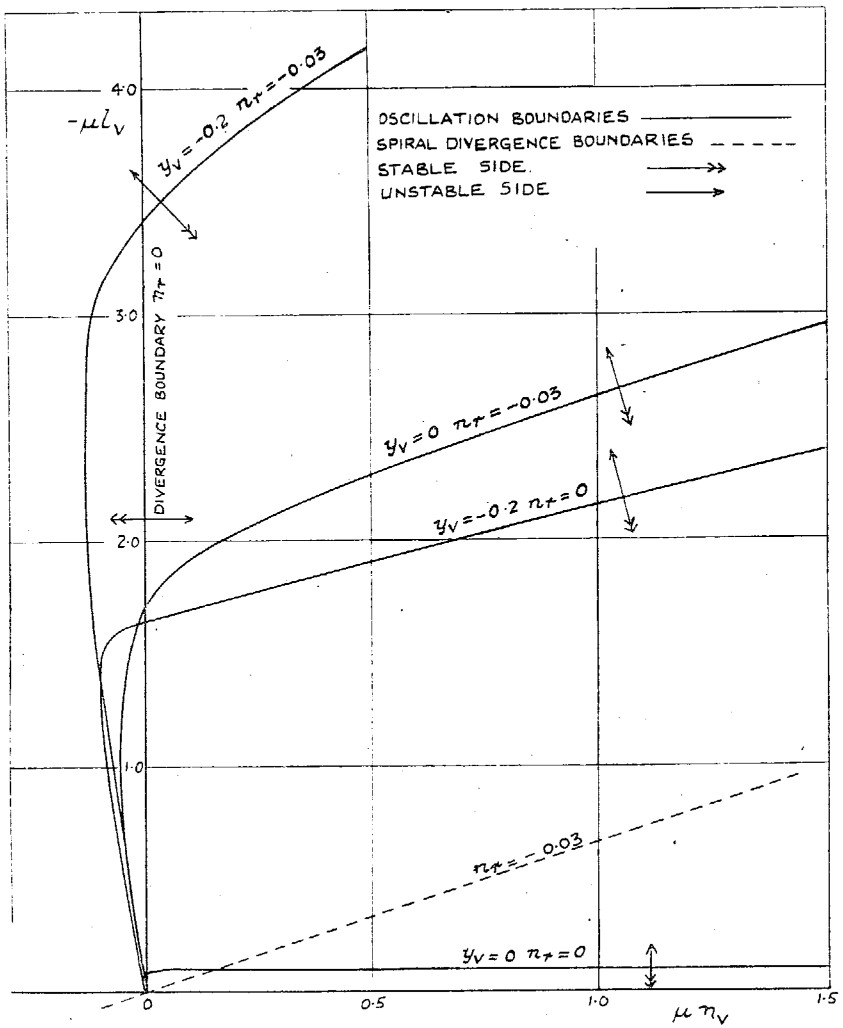


FIG. 3. Stability Boundaries $C_L = 0 \cdot 1$, $i_A = 0 \cdot 09$, $i_C = 0 \cdot 12$

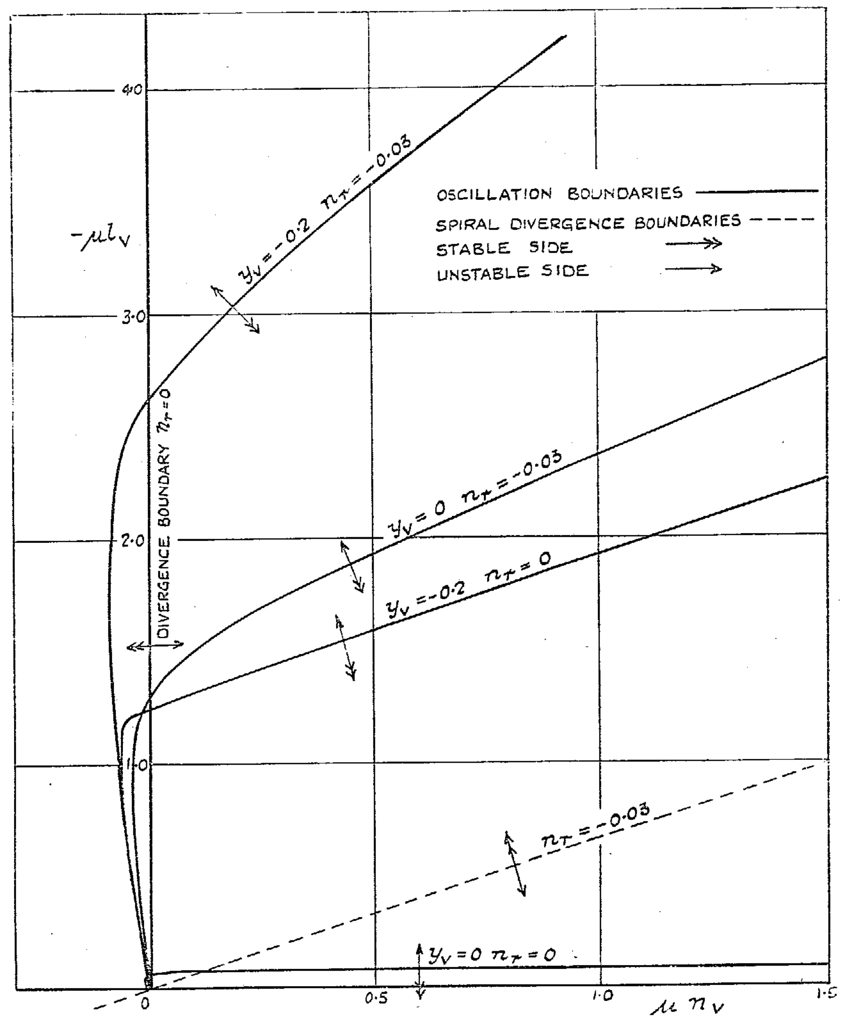


FIG. 4. Stability Boundaries $C_L = 0 \cdot 1$, $i_A = 0 \cdot 12$, $i_C = 0 \cdot 12$

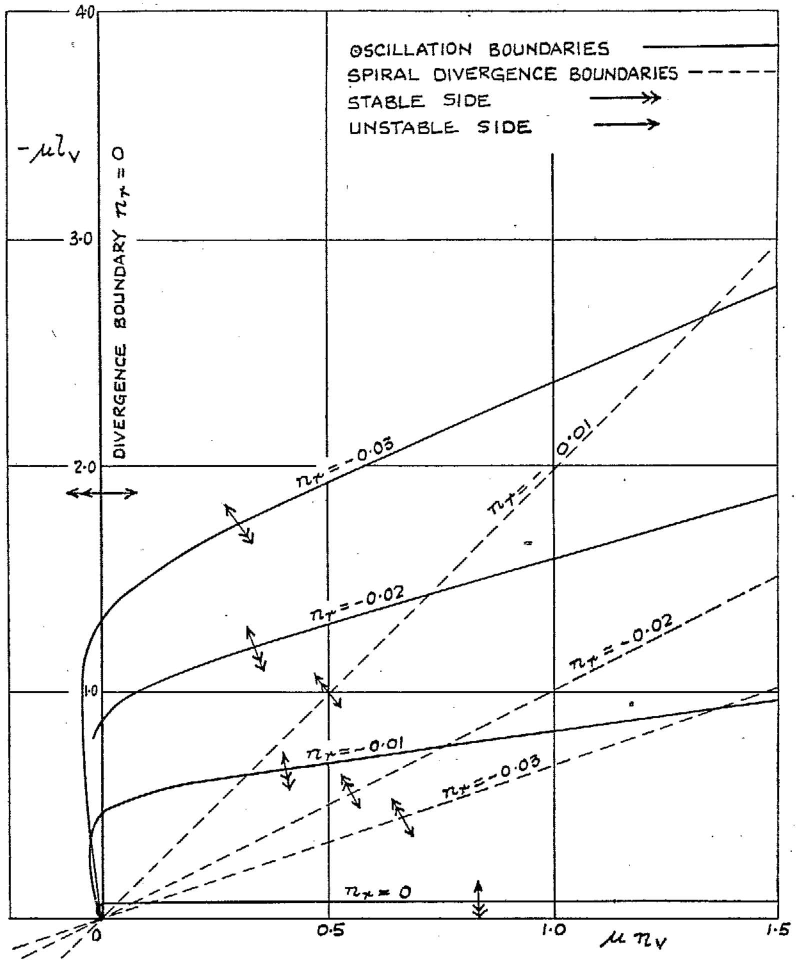


FIG. 5. Stability Boundaries $C_L = 0 \cdot 1$, $i_A = 0 \cdot 12$, $i_C = 0 \cdot 12$, $y_v = 0$

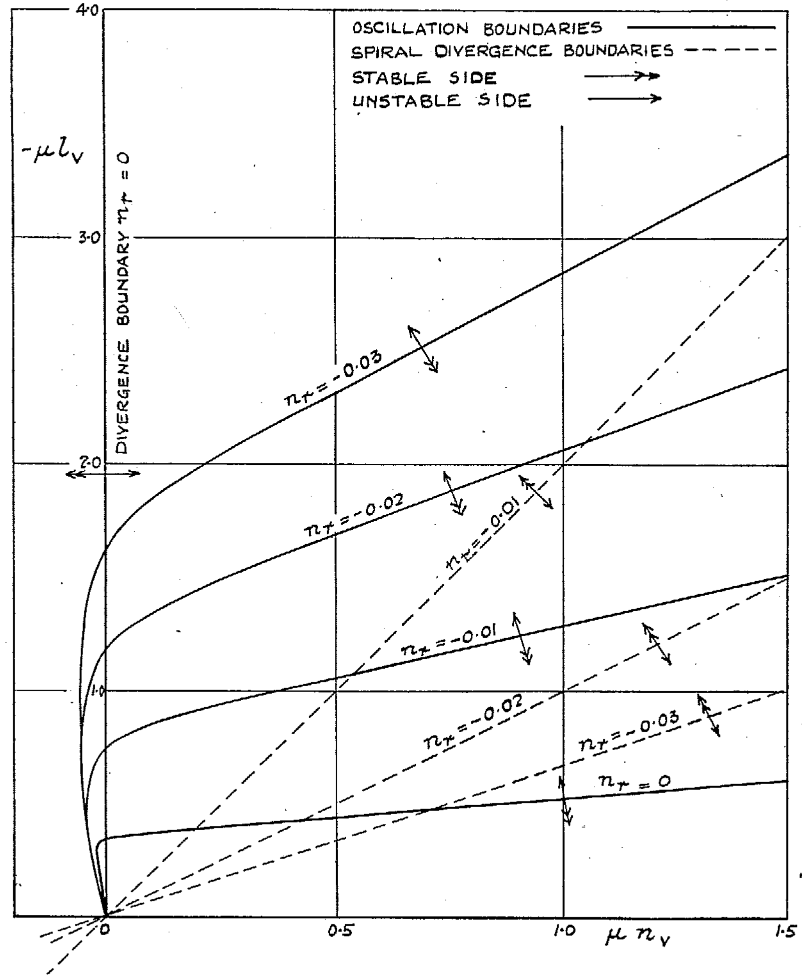


FIG. 6. Stability Boundaries $C_L = 0 \cdot 1$, $i_A = 0 \cdot 12$, $i_C = 0 \cdot 12$, $y_v = -0 \cdot 05$

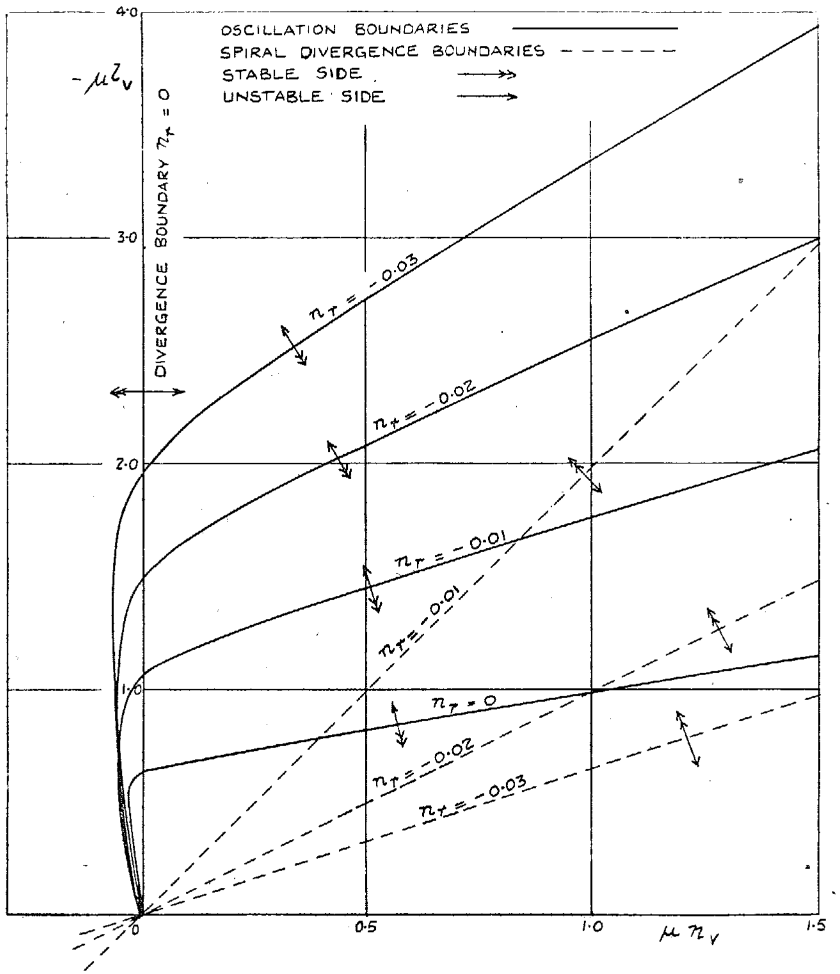


FIG. 7. Stability Boundaries $C_L = 0{\cdot}1$, $i_A = 0{\cdot}12$, $i_C = 0{\cdot}12$, $y_v = -0{\cdot}1$

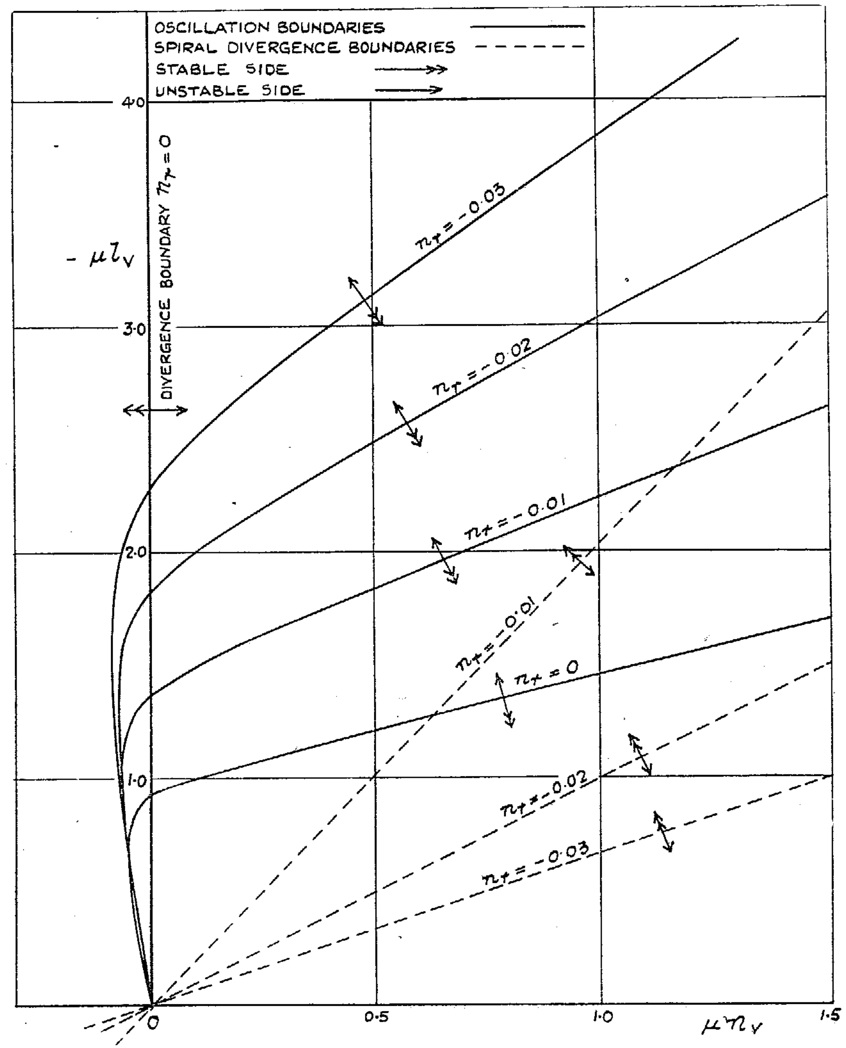


FIG. 8. Stability Boundaries $C_L = 0{\cdot}1$ $i_A = 0{\cdot}12$, $i_C = 0{\cdot}12$, $y_v = -0{\cdot}15$

(79728)

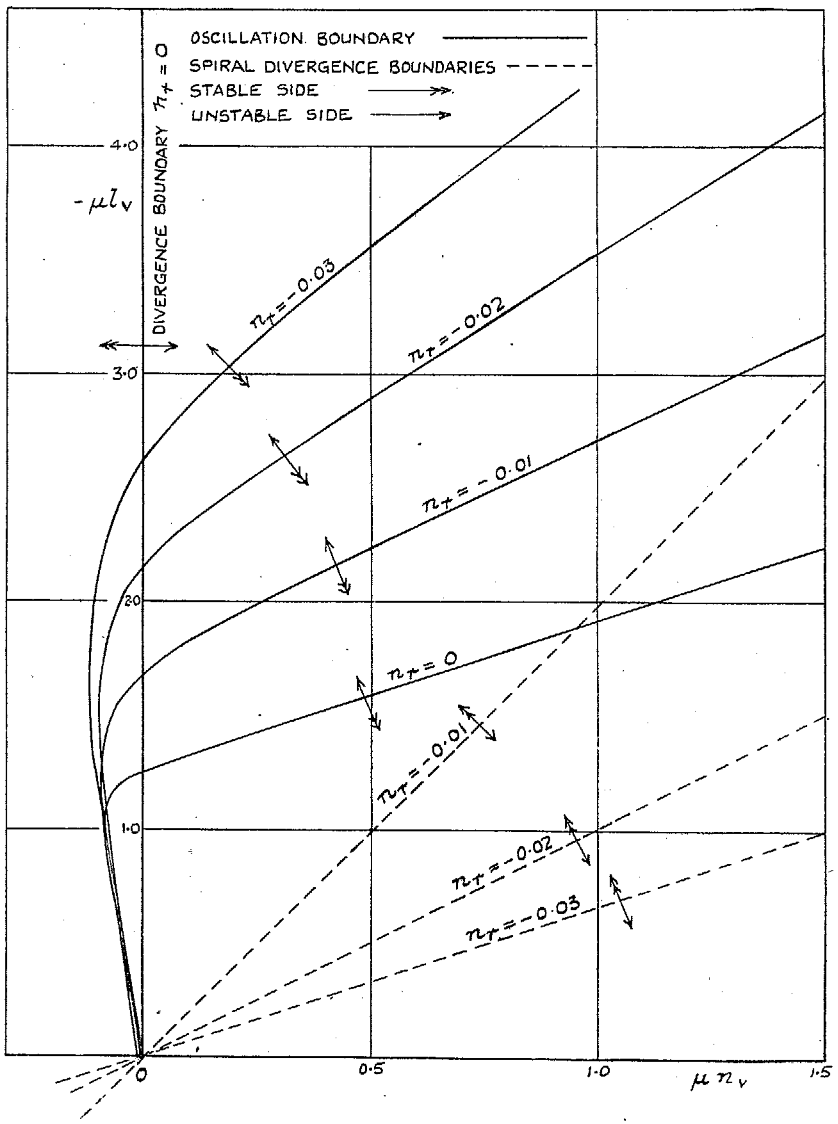


FIG. 9. Stability Boundaries $C_L = 0{\cdot}1$, $i_A = 0{\cdot}12$, $i_C = 0{\cdot}12$, $y_v = -0{\cdot}2$

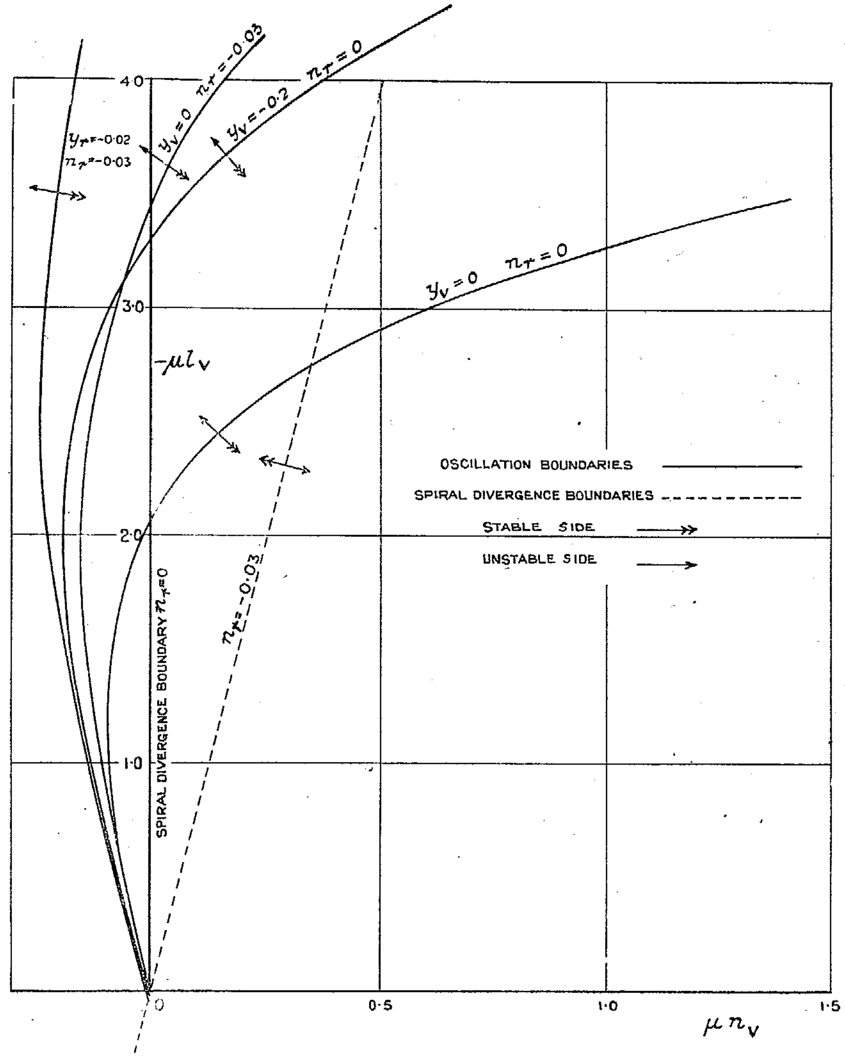


FIG. 10. Stability Boundaries $C_L = 1{\cdot}0$, $i_A = 0{\cdot}05$, $i_C = 0{\cdot}08$

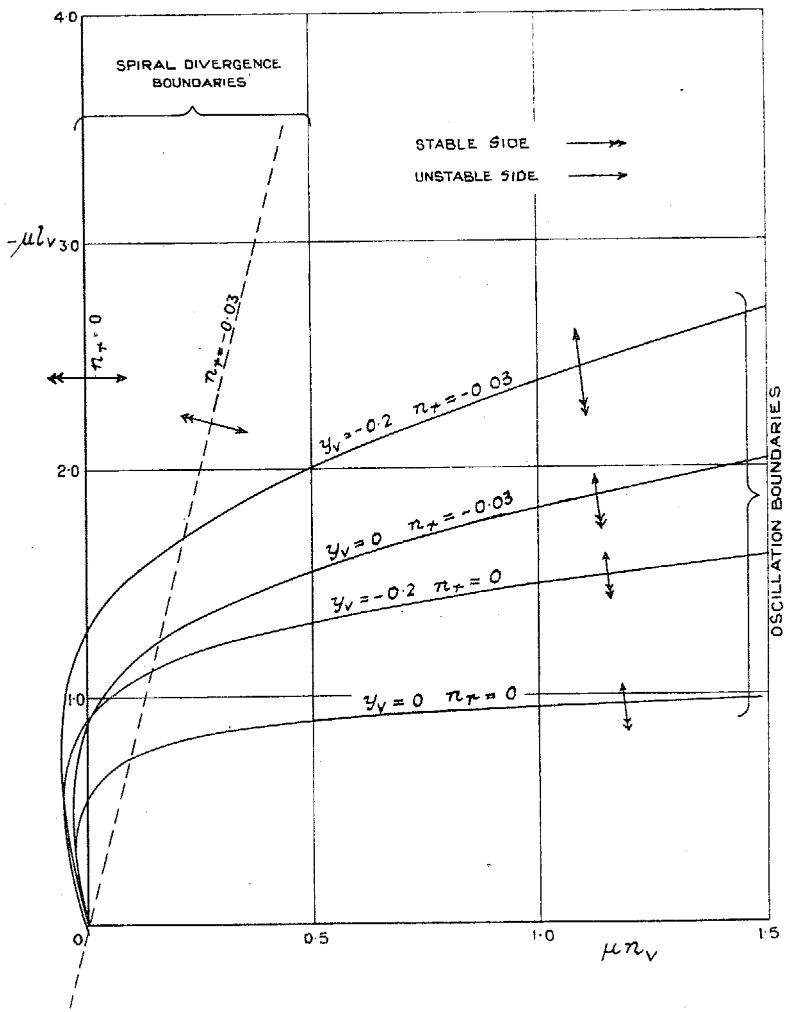


FIG. 11. Stability Boundaries $C_L = 1 \cdot 0$, $i_A = 0 \cdot 09$, $i_C = 0 \cdot 09$

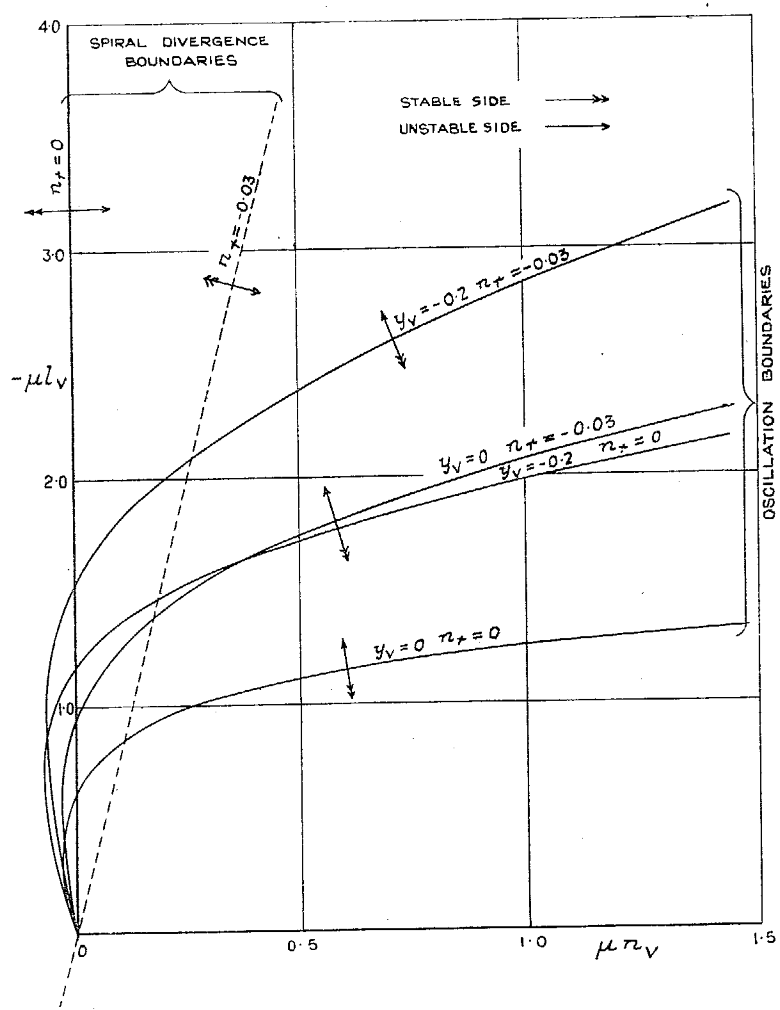


FIG. 12. Stability Boundaries $C_L = 1 \cdot 0$, $i_A = 0 \cdot 09$, $i_C = 0 \cdot 12$

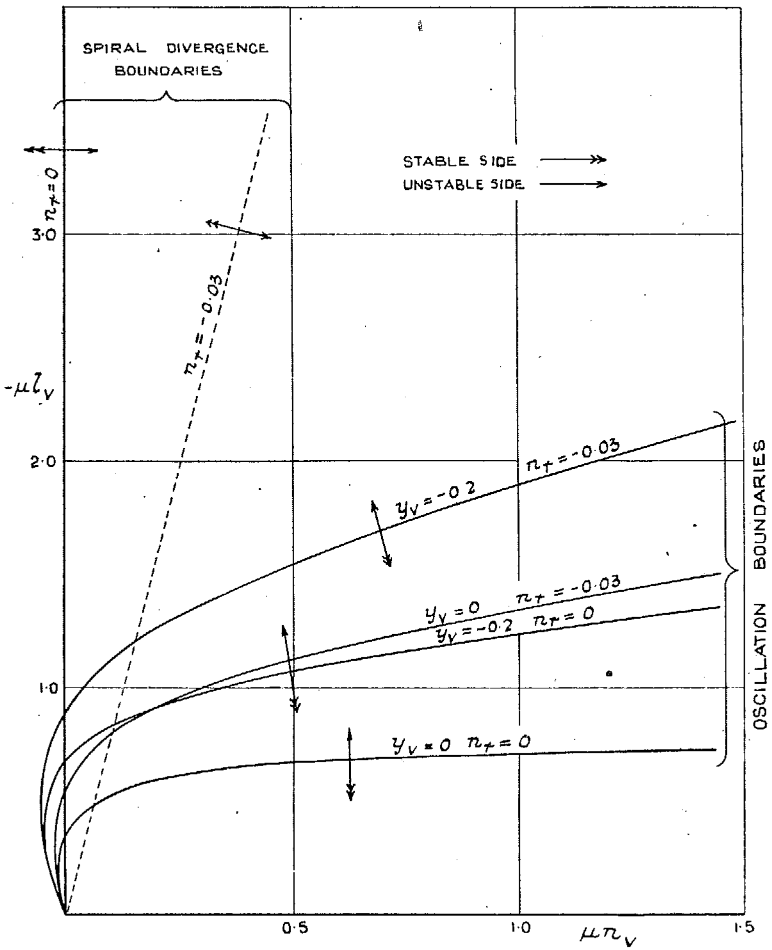


FIG. 13. Stability Boundaries $C_L = 1 \cdot 0$, $i_A = 0 \cdot 12$, $i_C = 0 \cdot 12$

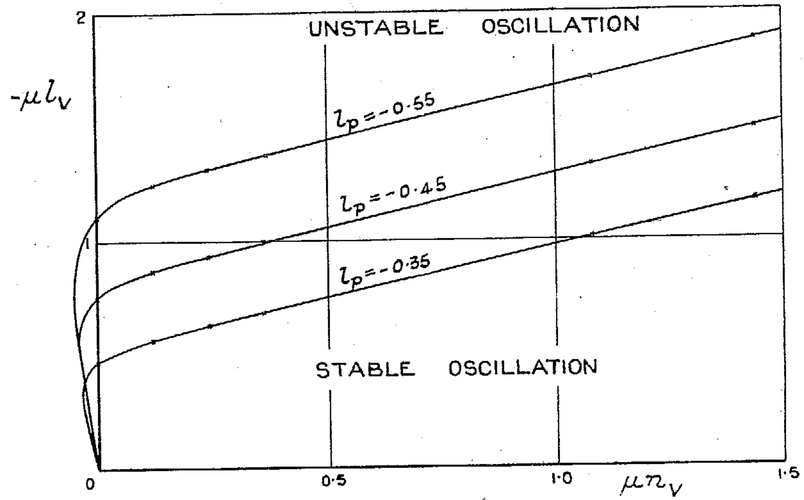


FIG. 14. Stability Boundaries $C_L = 0 \cdot 1$, $i_A = 0 \cdot 12$, $i_C = 0 \cdot 12$, $y_v = -0 \cdot 05$, $n_r = -0 \cdot 01$. Variation with $l_p$.

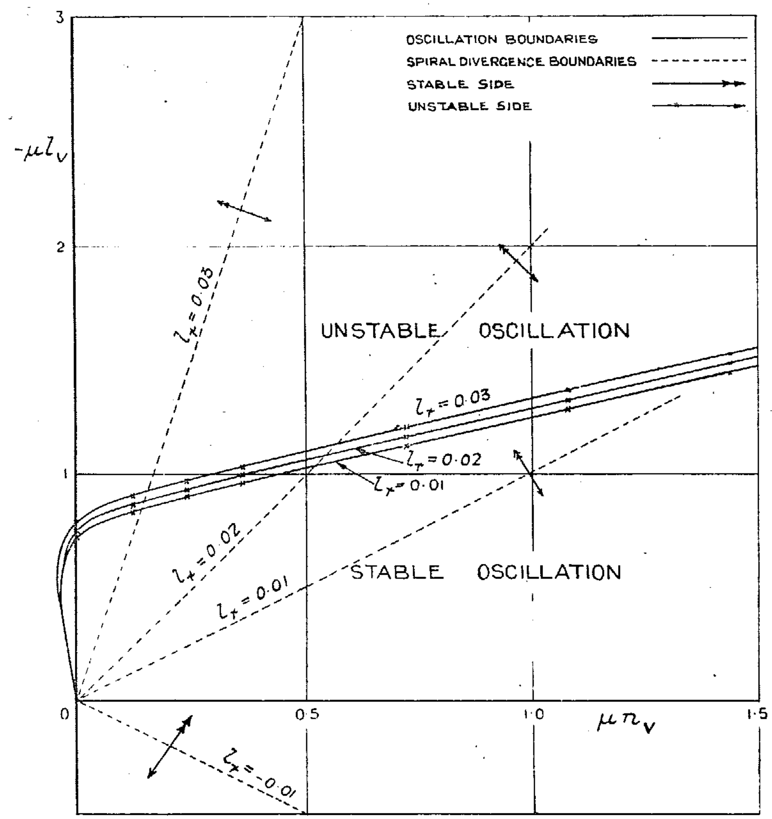


FIG. 15. Stability Boundaries $C_L = 0 \cdot 1$, $i_A = 0 \cdot 12$, $i_C = 0 \cdot 12$, $y_v = -0 \cdot 05$, $n_r = -0 \cdot 01$. Variation with $l_r$.

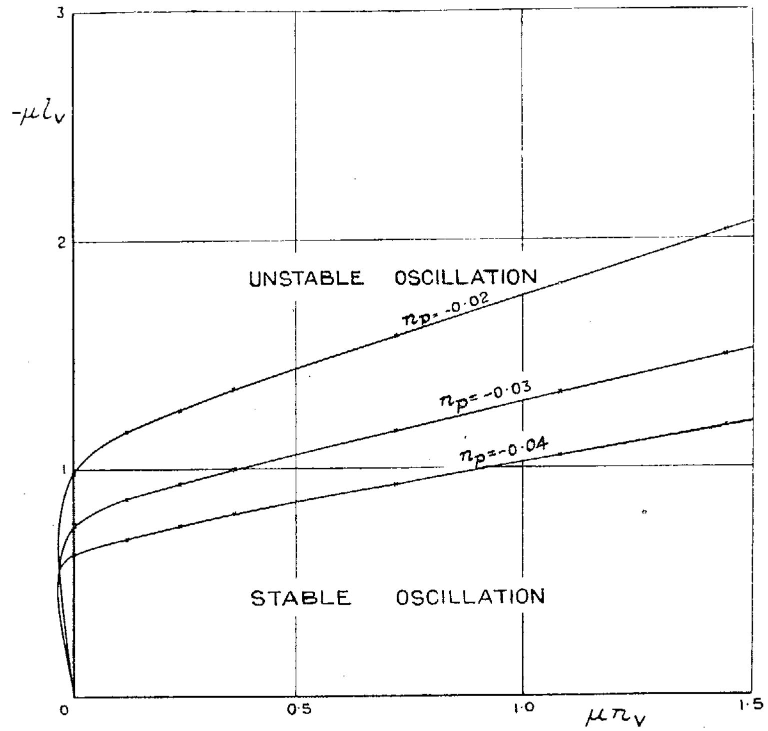


FIG. 16. Stability Boundaries $C_L = 0 \cdot 1$, $i_A = 0 \cdot 12$, $i_C = 0 \cdot 12$, $y_v = -0 \cdot 05$, $n_r = -0 \cdot 01$. Variation with $n_p$.

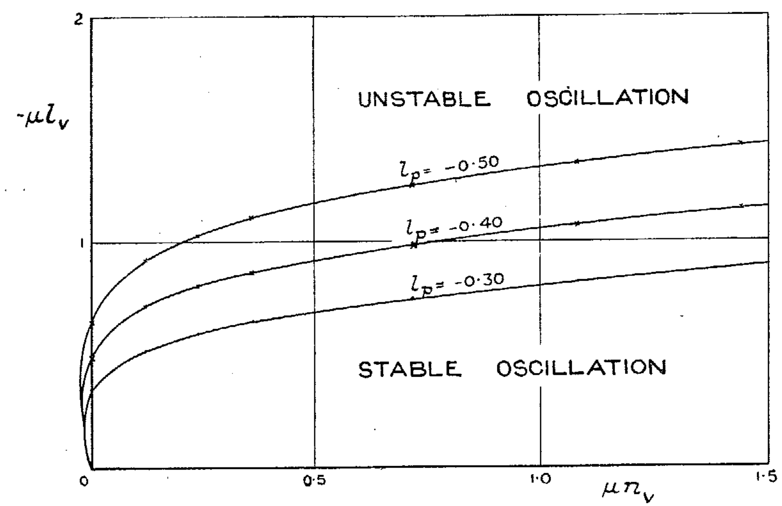


FIG. 17. Stability Boundaries $C_L = 1 \cdot 0$, $i_A = 0 \cdot 12$, $i_C = 0 \cdot 12$, $y_v = -0 \cdot 05$, $n_r = -0 \cdot 01$. Variation with $l_p$.

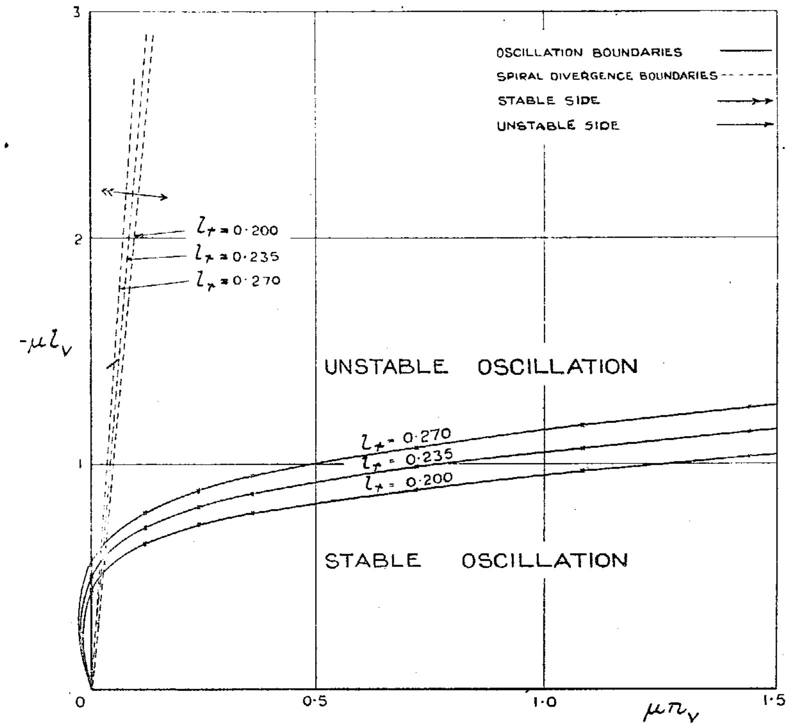


FIG. 18. Stability Boundaries $C_L = 1 \cdot 0$, $i_A = 0 \cdot 12$, $i_C = 0 \cdot 12$, $y_v = -0 \cdot 05$, $n_r = -0 \cdot 01$. Variation with $l_r$.

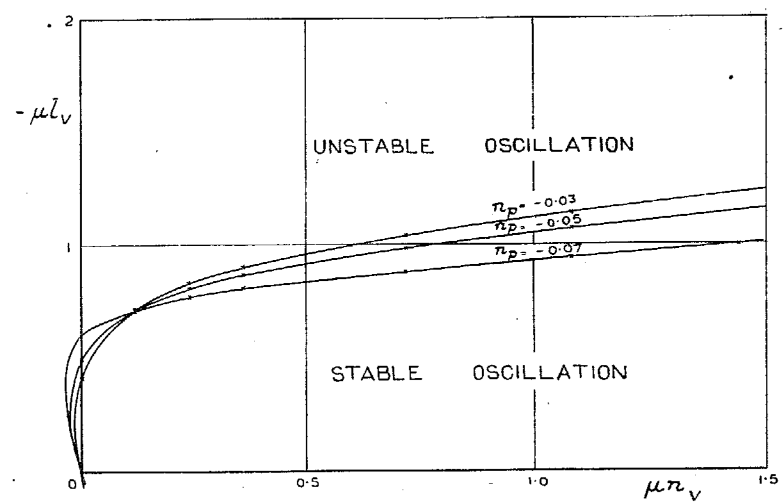


FIG. 19. Stability Boundaries $C_L = 1 \cdot 0$, $i_A = 0 \cdot 12$, $i_C = 0 \cdot 12$, $y_v = -0 \cdot 05$, $n_r = -0 \cdot 01$. Variation with $n_p$.

(79722)

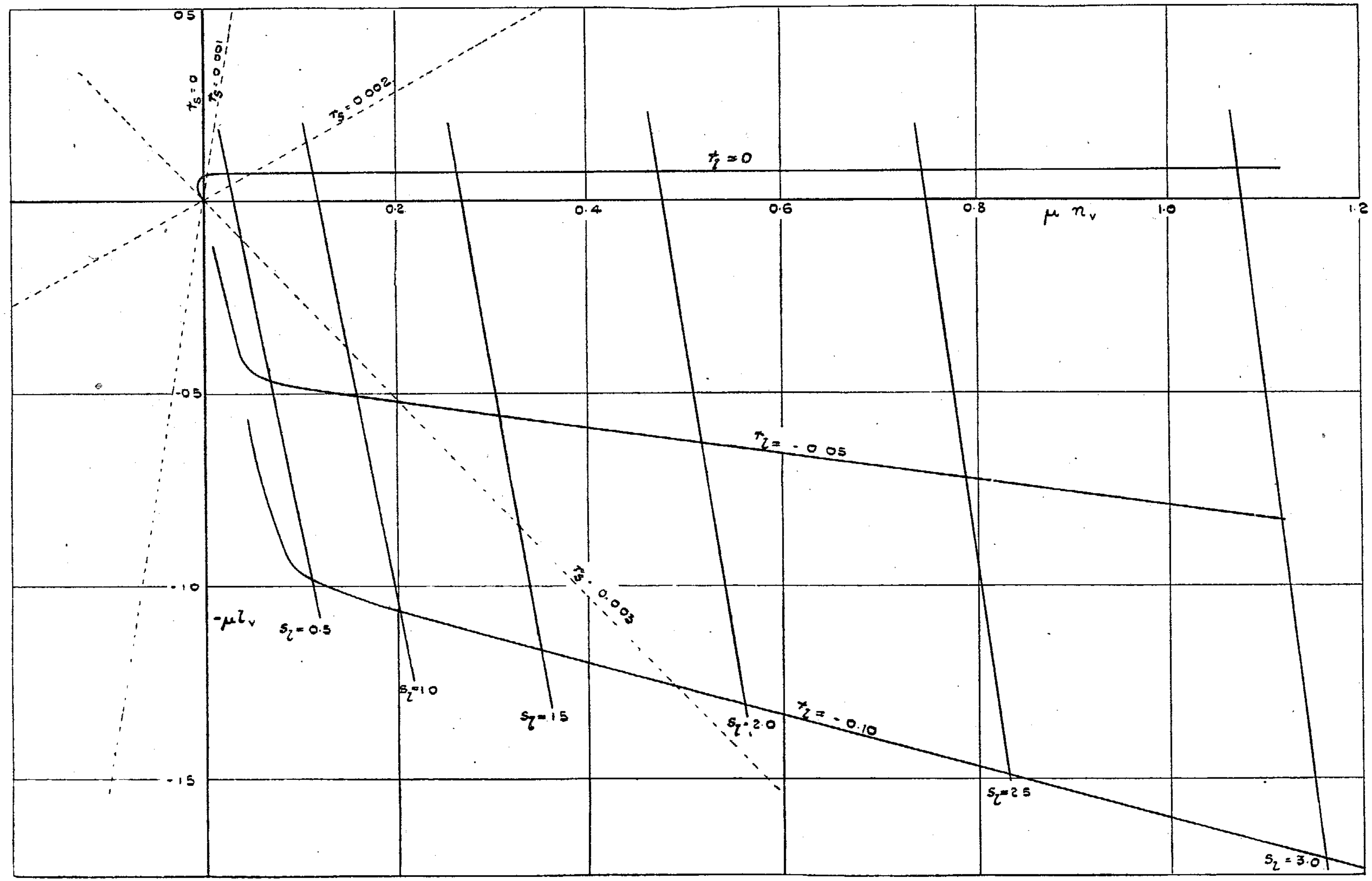


$r_l$ and $s_l$ are the damping and frequency coefficients of the oscillatory motion.
$r_s$ is the damping coefficient of the "spiral" motion.

FIG. 20. Frequency and Damping Coefficients $C_L = 0 \cdot 1$, $i_A = 0 \cdot 12$, $i_C = 0 \cdot 12$, $y_v = 0$, $n_r = 0$.

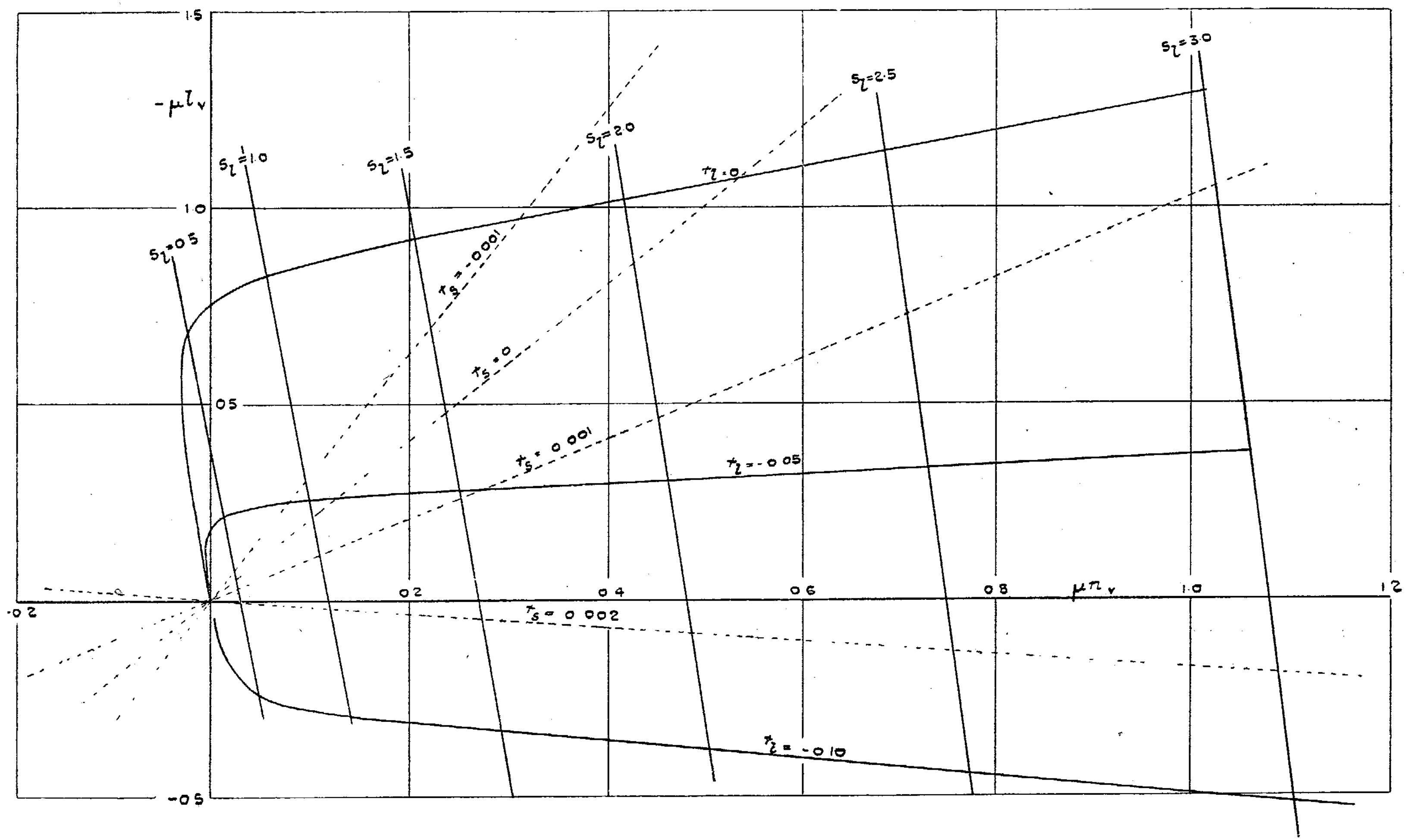


$r_l$ and $s_l$ are the damping and frequency coefficients of the oscillatory motion.

$r_s$ is the damping coefficient of the "spiral" motion.

FIG. 21. Frequency and Damping Coefficients $C_L = 0 \cdot 1$, $i_A = 0 \cdot 12$, $i_C = 0 \cdot 12$, $y_v = -0 \cdot 05$, $n_r = -0 \cdot 01$.

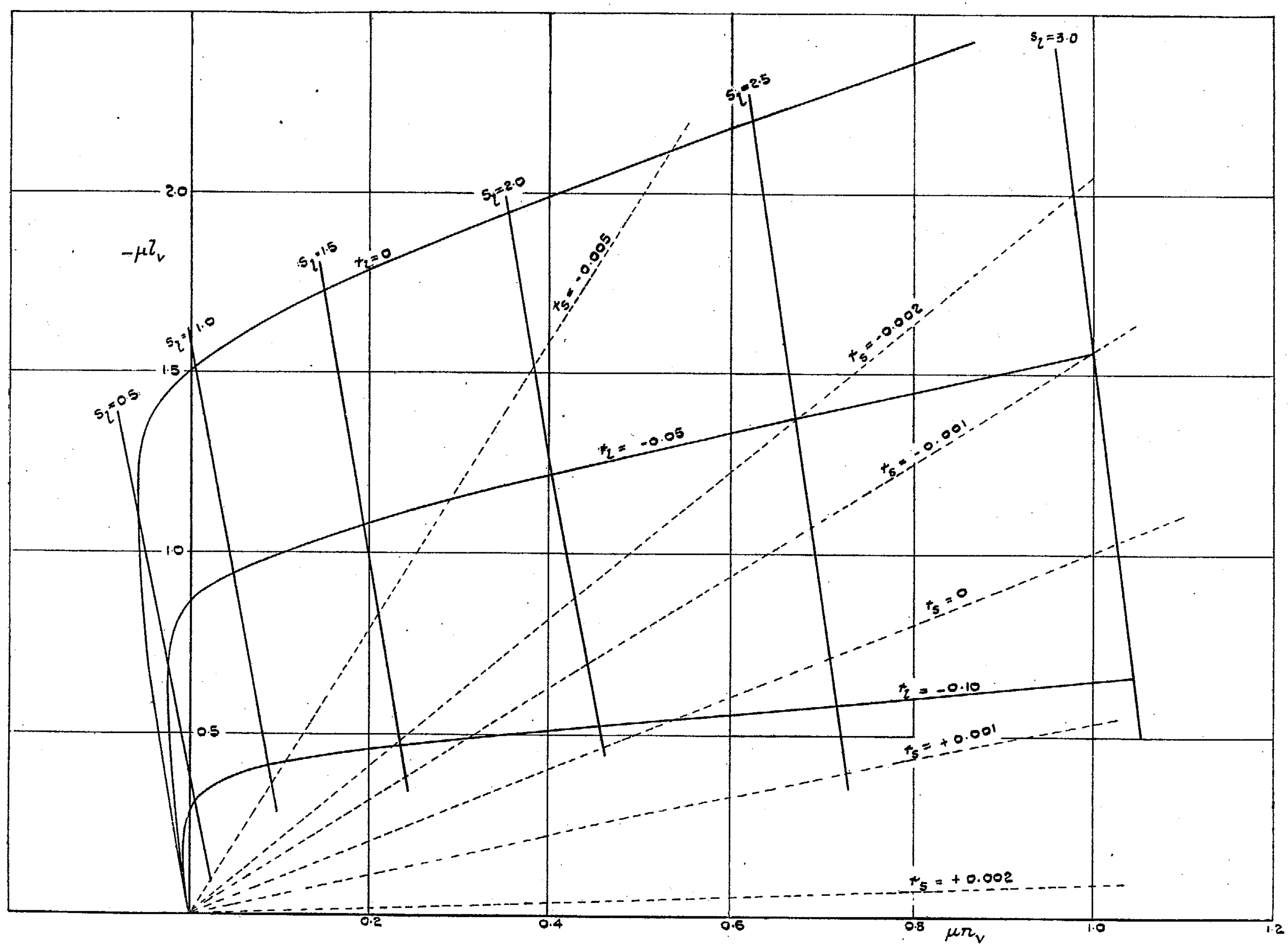


$r_l$ and $s_l$ are the damping and frequency coefficients of the oscillatory motion.
$r_s$ is the damping coefficient of the "spiral" motion.

FIG. 22. Frequency and Damping Coefficients $C_L = 0 \cdot 1$, $i_A = 0 \cdot 12$, $i_C = 0 \cdot 12$, $y_v = -0 \cdot 10$, $n_r = -0 \cdot 02$.

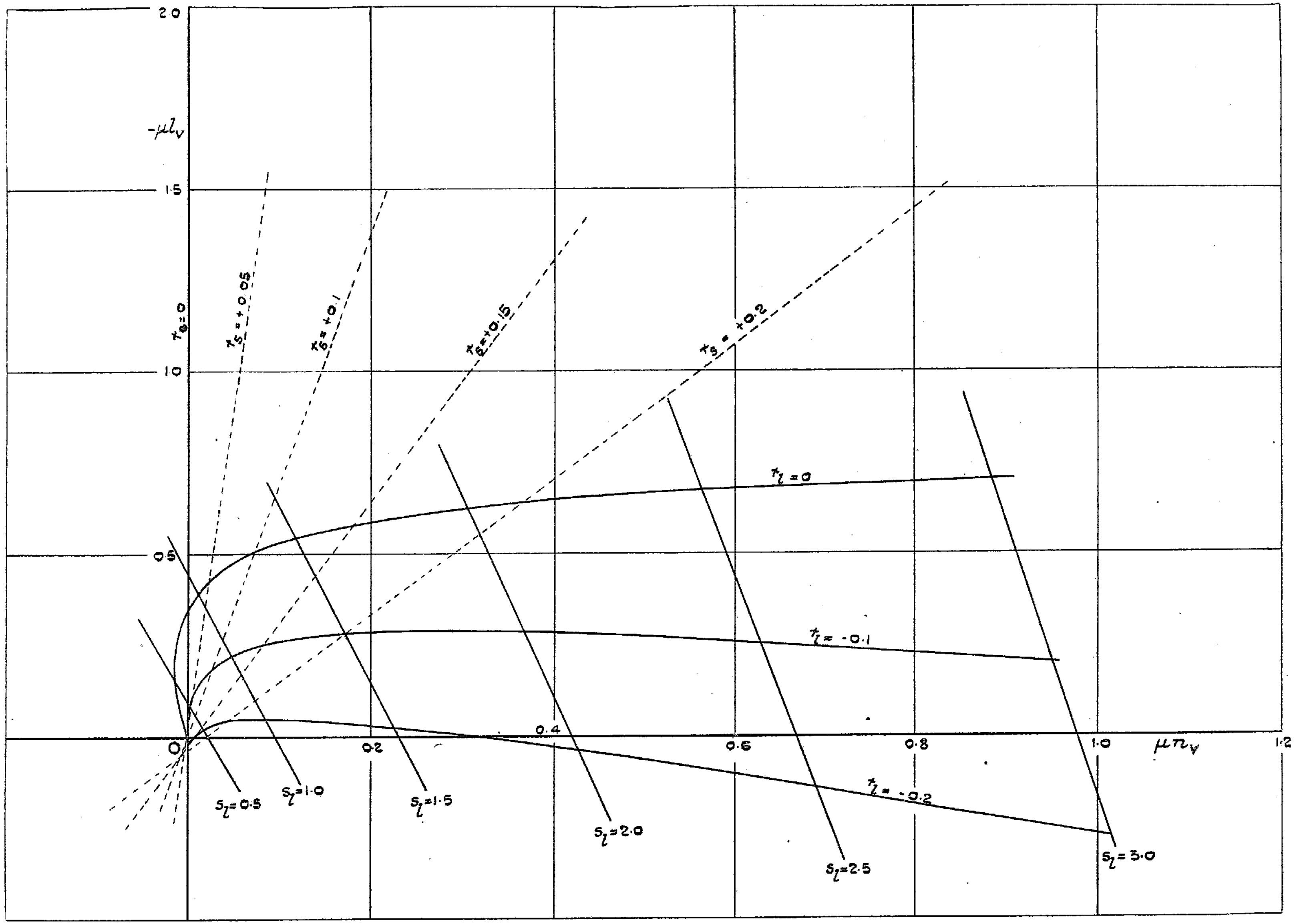


$r_l$ and $s_l$ are the damping and frequency coefficients of the oscillatory motion.
$r_s$ is the damping coefficient of the "spiral" motion.

FIG. 23. Frequency and Damping Coefficients $C_L = 1·0$, $i_A = 0·12$, $i_C = 0·12$, $y_v = 0$, $n_r = 0$.

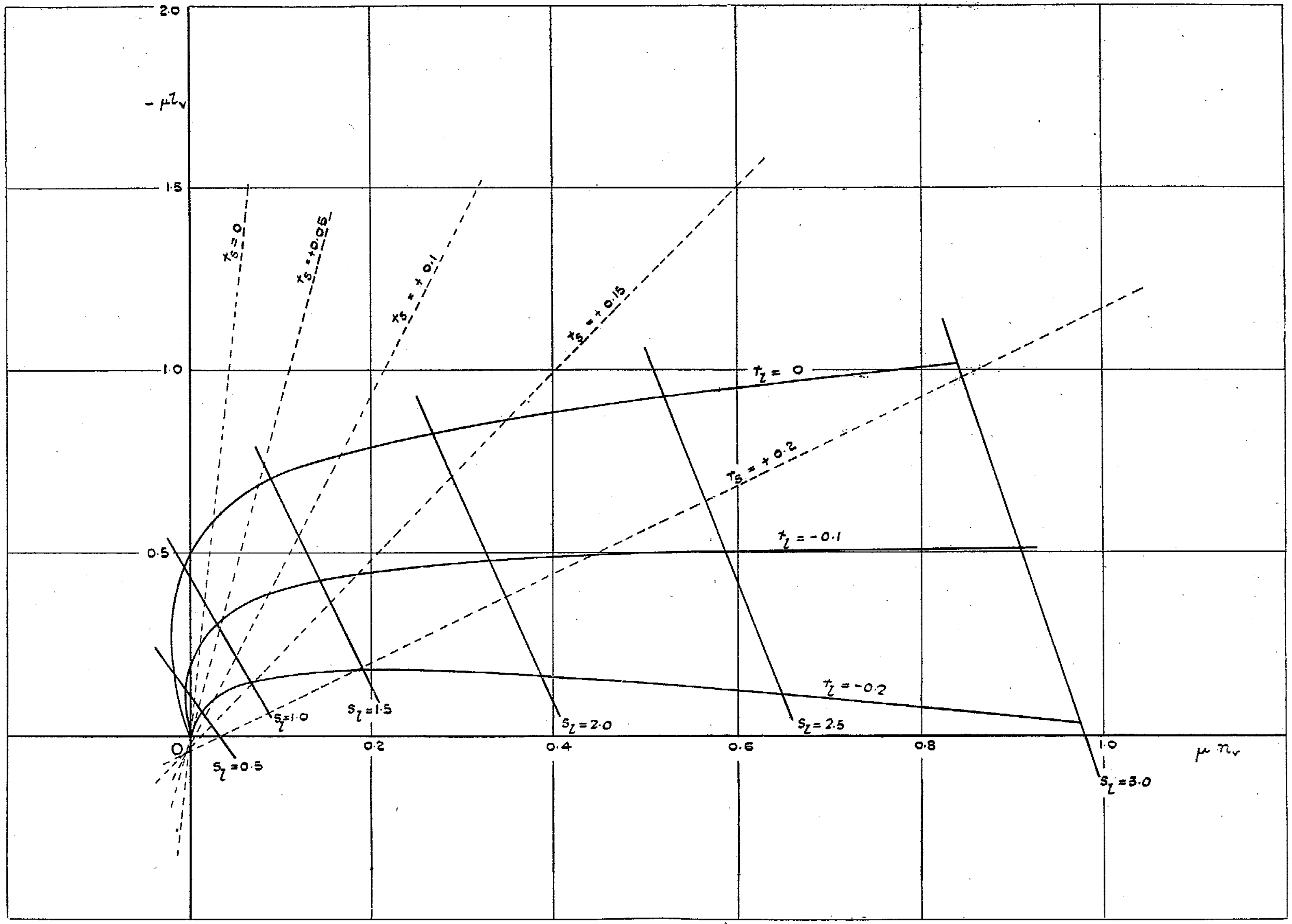


$r_l$ and $s_l$ are the damping and frequency coefficients of the oscillatory motion.
$r_s$ is the damping coefficient of the "spiral" motion.

FIG. 24. Frequency and Damping Coefficients $C_L = 1 \cdot 0$, $i_A = 0 \cdot 12$, $i_C = 0 \cdot 12$, $y_v - 0 \cdot 05$, $n_r = -0 \cdot 01$.

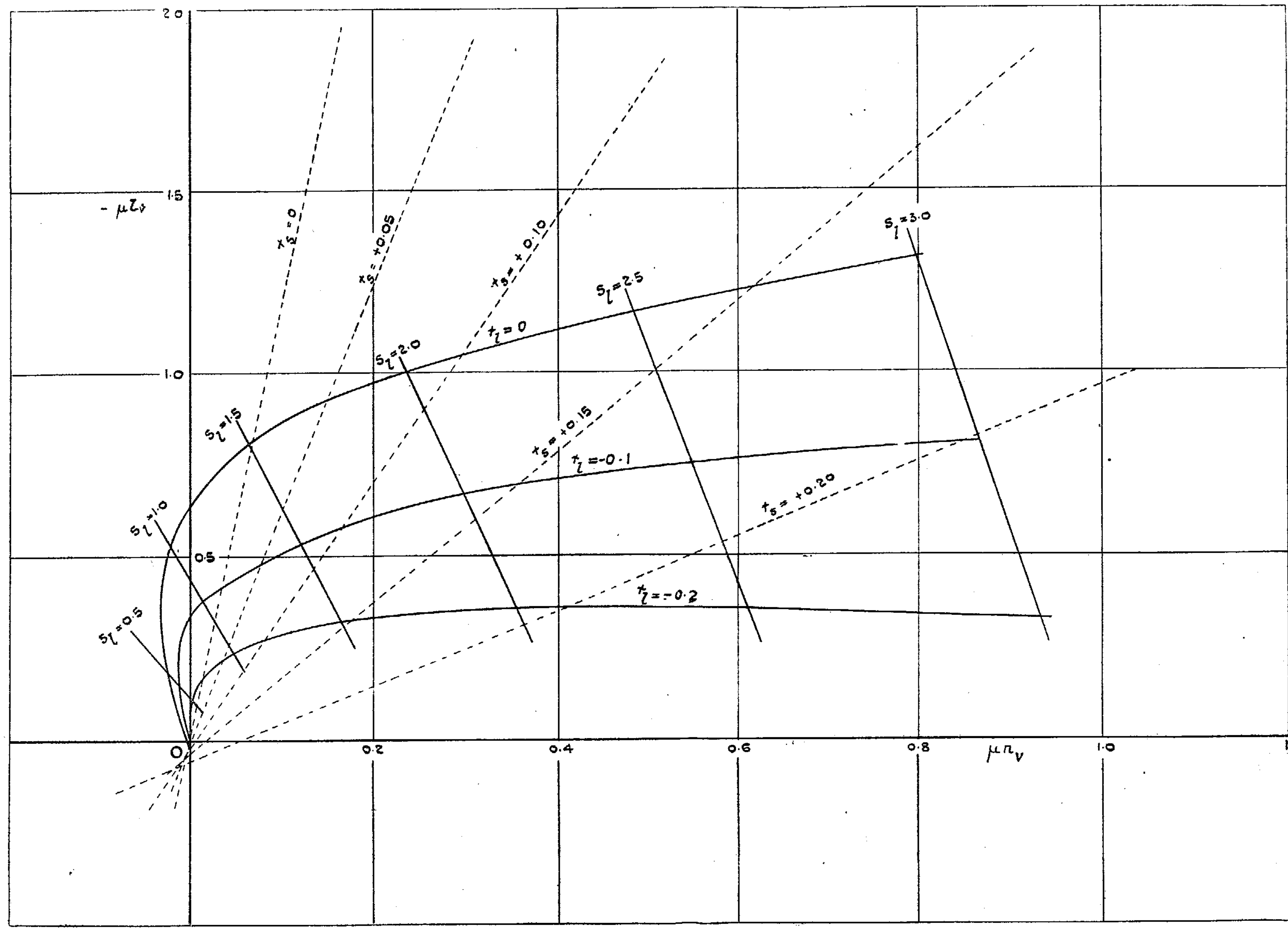


$r_l$ and $s$ are the damping and frequency coefficients of the oscillatory motion.
$r_s$ is the damping coefficient of the "spiral" motion.

FIG. 25. Frequency and Damping Coefficients $C_L = 1\cdot0$, $i_A = 0\cdot12$, $i_C = 0\cdot12$, $y_v = -0\cdot1$, $n_r = -0\cdot02$.

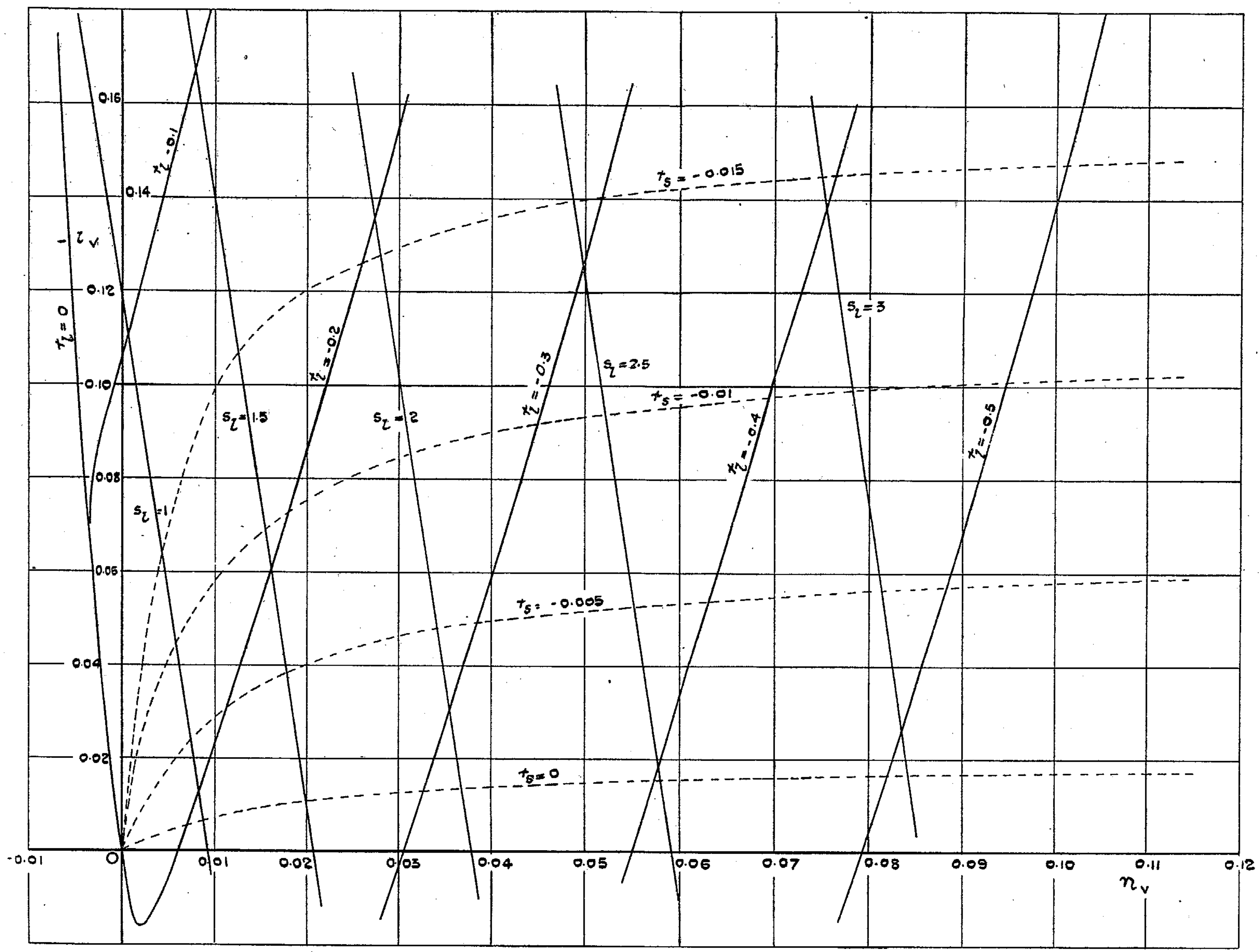


$r_l$ and $s$ are the damping and frequency coefficients of the oscillatory motion.
$r_s$ is the damping coefficient of the "spiral" motion.

FIG. 26. Frequency and Damping Coefficients (Conventional Aircraft) $C_L = 0{\cdot}1$, $\mu = 13$, $i_A = 0{\cdot}0625$, $i_c = 0{\cdot}1225$

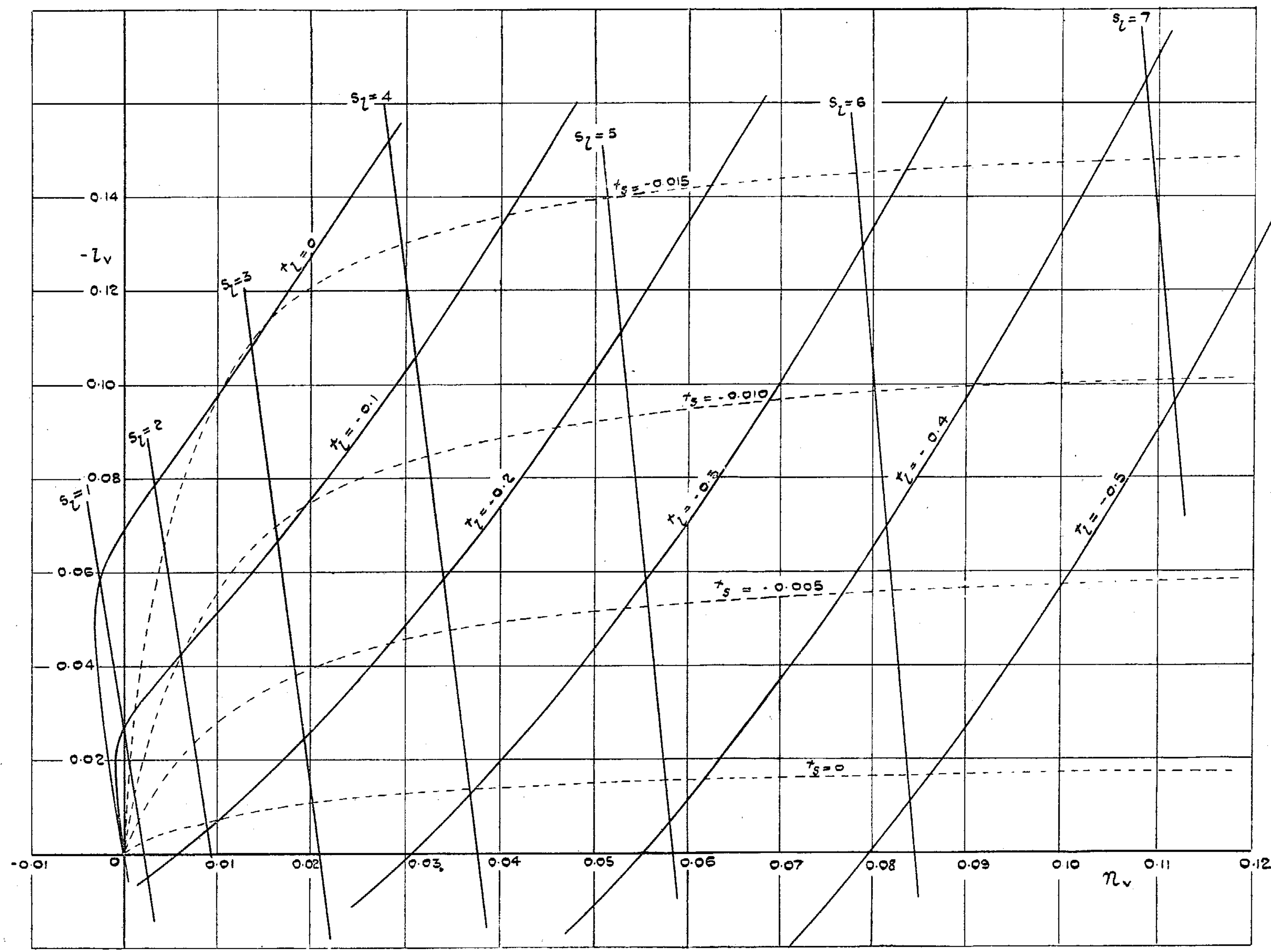


$r_l$ and $s_l$ are the damping and frequency coefficients of the oscillatory motion.
$r_s$ is the damping coefficient of the "spiral" motion.

FIG. 27. Frequency and Damping Coefficients (Conventional Aircraft) $C_L = 0 \cdot 1$, $\mu = 52$, $i_A = 0 \cdot 0625$, $i_C = 0 \cdot 1225$.

(79722) Wt. 11 12/47 Hw.

R. & M. No. 2074
(6932)
A.R.C. Technical Report

# Publications of the Aeronautical Research Committee

TECHNICAL REPORTS OF THE AERONAUTICAL RESEARCH COMMITTEE—

1934-35 Vol. I. Aerodynamics. 40*s.* (40*s.* 8*d.*)
Vol. II. Seaplanes, Structures, Engines, Materials, etc. 40*s.* (40*s.* 8*d.*)

1935-36 Vol. I. Aerodynamics. 30*s.* (30*s.* 7*d.*)
Vol. II. Structures, Flutter, Engines, Seaplanes, etc. 30*s.* (30*s.* 7*d.*)

1936 Vol. I. Aerodynamics General, Performance, Airscrews, Flutter and Spinning. 40*s.* (40*s.* 9*d.*)
Vol. II. Stability and Control, Structures, Seaplanes, Engines, etc. 50*s.* (50*s.* 10*d.*)

1937 Vol. I. Aerodynamics General, Performance, Airscrews, Flutter and Spinning. 40*s.* (40*s.* 9*d.*)
Vol. II. Stability and Control, Structures, Seaplanes Engines, etc. 60*s.* (61*s.*)

ANNUAL REPORTS OF THE AERONAUTICAL RESEARCH COMMITTEE—

1933-34 1*s.* 6*d.* (1*s.* 8*d.*)
1934-35 1*s.* 6*d.* (1*s.* 8*d.*)
April 1, 1935 to December 31, 1936. 4*s.* (4*s.* 4*d.*)
1937 2*s.* (2*s.* 2*d.*)
1938 1*s.* 6*d.* (1*s.* 8*d.*)

INDEXES TO THE TECHNICAL REPORTS OF THE ADVISORY COMMITTEE ON AERONAUTICS—

December 1, 1936 — June 30, 1939
Reports & Memoranda No. 1850. 1*s.* 3*d.* (1*s.* 5*d.*)
July 1, 1939 — June 30, 1945
Reports & Memoranda No. 1950. 1*s.* (1*s.* 2*d.*)

*Prices in brackets include postage.*

Obtainable from

## His Majesty's Stationery Office

London W.C.2: York House, Kingsway
[Post Orders—P.O. Box No. 569, London, S.E.1.]
Edinburgh 2: 13A Castle Street — Manchester 2: 39-41 King Street
Cardiff: 1 St. Andrew's Crescent — Bristol 1: Tower Lane
Belfast: 80 Chichester Street
or through any bookseller.

S.O. Code No. 23-2074